NATIONAL ADVISORY COMMITTEE FOR AERONAUTICS

TECHNICAL NOTE 4193

SUBSONIC FLIGHT INVESTIGATION OF METHODS TO IMPROVE THE DAMPING OF LATERAL OSCILLATIONS BY MEANS OF A VISCOUS DAMPER IN THE RUDDER SYSTEM IN CONJUNCTION WITH ADJUSTED HINGE-MOMENT PARAMETERS

By Harold L. Crane, George J. Hurt, Jr., and John M. Elliott

Langley Aeronautical Laboratory
Langley Field, Va.

Washington
January 1958

NATIONAL ADVISORY COMMITTEE FOR AERONAUT

TECHNICAL NOTE 4193

SUBSONIC FLIGHT INVESTIGATION OF METHODS TO IMPROVE THE DAMPING OF LATERAL OSCILLATIONS BY MEANS OF A VISCOUS DAMPER IN THE RUDDER SYSTEM IN CONJUNCTION WITH ADJUSTED HINGE-MOMENT PARAMETERS[1]

By Harold L. Crane, George J. Hurt, Jr., and John M. Elliott

SUMMARY

A flight investigation at subsonic speeds of a method to improve the damping of lateral oscillations by means of a viscous damping cylinder used in the rudder system in conjunction with adjusted hinge-moment parameters has been conducted at the Langley Aeronautical Laboratory. The damping device has been applied to a modern fighter-type jet-powered airplane. The rudder was made to float with the relative wind by the addition of trailing-edge strips. In order to amplify the floating tendency (by reducing the restoring moment), a highly geared balancing tab was incorporated. Lag of the motion of the free rudder with respect to the yawing of the airplane was introduced by means of a small viscous damping cylinder linked to the rudder.

Several configurations of the damping device have been tested and it was found that the better ones increased the damping of the airplane with rudder free so that the number of cycles to damp to one-half amplitude decreased from 2 to 3 for the production configuration to 0.5 to 1.5 with damping augmenter installed. The tests were conducted at altitudes of 10,000 and 30,000 feet at Mach numbers from approximately 0.35 to approximately 0.75.

This paper presents and discusses the measured damping and hinge-moment data for several test configurations and also discusses briefly related problems which may result from the application of such a viscous damping device.

---

[1]Supersedes recently declassified NACA Research Memorandum L54D09 by Harold L. Crane, George J. Hurt, Jr., and John M. Elliott, 1954.

INTRODUCTION

The aerodynamic damping of the lateral oscillations of modern high-performance aircraft has tended to be deficient. This deficiency has sometimes not been discovered until after the design of the aerodynamic configuration has been frozen. In other cases, the poor damping has been predicted but could not be corrected by reasonable changes in the design. It would, therefore, be desirable to have augmenters available for lateral damping that do not require major changes in the aerodynamic configuration. Although electronic devices have been developed for use as lateral dampers, it has been suggested that mechanical devices could be developed for the same purpose that would tend to be simpler, more reliable, and less expensive. Various approaches to the problem have been tried and reported. For example, reference 1 presents flight results dealing with the effect of variation in rudder hinge-moment parameters on the damping of controls-free lateral oscillations.

If the rudder is freed during a lateral oscillation, it may either increase or decrease the rate of damping of the oscillation. Frequent instances have occurred where the combination of a control surface that tended to float against the relative wind with more than a minimum amount of friction has resulted in snaking oscillations, that is, oscillations which were reinforced by aerodynamic moments induced by the floating characteristics of the control surface. A tendency for the control to float against the relative wind (positive rudder floating parameter $C_{h_{\alpha_t}}$) causes reinforcement of the oscillation; a tendency for the control to float with the relative wind (negative $C_{h_{\alpha_t}}$) increases the damping. In order to increase the damping, lag must be introduced by means of friction, inertia, or viscous effects. Since static friction would cause the rudder to remain fixed below a certain amplitude, friction must be of the viscous type if an improvement of the damping at very small amplitudes is desired. These effects are explained in reference 2, which is a theoretical analysis of the influence of rudder hinge-moment parameters and control-system friction on the damping of controls-free lateral oscillations.

The Langley Flight Research Division has been investigating the practicability of using a small viscous damping cylinder in the rudder system in conjunction with adjusted hinge-moment parameters in order to cause the rudder to float with the relative wind, to lag the sideslip angle and thereby to reinforce the damping of the controls-free lateral oscillation. An unswept-wing jet fighter which has unsatisfactory damping characteristics has been used as a test vehicle. A single-degree-of-freedom theoretical analysis was made to provide a guide for the variation of the parameters. The hinge-moment parameters were adjusted by changes in tab gearing and the use of trailing-edge strips. The data of reference 3 and unpublished data were used as a guide to determine the approximate effect of trailing-edge strips on rudder

hinge-moment parameters. Tab effectiveness was measured in flight and tab hinge moments were estimated.

During the present investigation the measurements of the effectiveness of the damping augmenter have been made with the rudder pedals free. However, the principal value of such a device would, in practice, be for use in such maneuvers as strafing runs in which the controls are partially restrained by the pilot. For this reason, some measurements in strafing runs and in flight through rough air were attempted.

This paper presents a comparison of the lateral damping with and without three versions of the viscous damping device as well as data concerning the measured sideslip characteristics of the airplane and the hinge-moment parameters of the rudder.

SYMBOLS

The positive directions of the forces, moments, and angular displacements are shown in figure 1. The coefficients and symbols are defined as follows:

α_t angle of attack of vertical tail, deg

β angle of sideslip, deg

ψ angle of yaw, which is equal and opposite to the angle of sideslip if the system is assumed to have one degree of freedom, deg

δ rudder deflection, deg

N yawing moment

N_ψ rate of change of yawing moment with angle of yaw, ft-lb/radian

$N_{\dot{\psi}}$ rate of change of yawing moment with yawing velocity, ft-lb/radian/sec

N_δ rate of change of yawing moment with control (rudder) deflection, ft-lb/radian

I moment of inertia of airplane (about yawing axis), slug-ft^2

I_r moment of inertia of rudder about rudder hinge line, slug-ft^2

l tail length, ft; longitudinal distance is measured parallel to fuselage reference line from airplane center of gravity to 25-percent mean aerodynamic chord of vertical tail

ϕ angle of bank, deg

L rolling moment

α angle of attack of fuselage center line, deg

V true airspeed, fps

V_i indicated airspeed, knots

H_{α_t} rate of change of rudder hinge moment with angle of attack of vertical tail, ft-lb/deg

H_δ rate of change of rudder hinge moment with rudder deflection, ft-lb/deg

$H_{\dot{\delta}}$ rate of change of rudder hinge moment with time rate of change of rudder deflection, ft-lb/radian/sec

$C_{h_{\alpha_t}}$ rate of change of rudder hinge-moment coefficient with angle of attack of vertical tail per degree where $C_{h_{\alpha_t}} = \frac{H_{\alpha_t}}{qbc^2}$

C_{h_δ} rate of change of rudder hinge-moment coefficient with rudder deflection per degree where $C_{h_\delta} = \frac{H_\delta}{qbc^2}$

$C_{h_{\dot{\delta}}}$ rate of change of rudder hinge-moment coefficient with time rate of change of rudder deflection per radian per second where $C_{h_{\dot{\delta}}} = \frac{H_{\dot{\delta}}}{qbc^2}$

q dynamic pressure, lb/sq ft

b rudder span, ft

c root-mean-square chord of rudder, ft

d logarithmic decrement of lateral oscillation, where $d = \frac{0.693P}{T_{1/2}} = \frac{0.693}{N_{1/2}}$

ω_n airplane undamped natural frequency, radians/second

ζ ratio of actual damping to critical damping of uncontrolled airplane

D	differential operator, d/dt
h_p	pressure altitude
t	time, sec
P	period of oscillation, sec
P_n	undamped natural period of oscillation with rudder fixed, sec
$T_{1/2}$	time to damp to half amplitude, sec
$N_{1/2}$	cycles to damp to one-half amplitude
M	Mach number
X,Y,Z	coordinate axes

$$\tau = \frac{H_{\dot{\delta}}}{H_{\delta}} \text{ or } \frac{C_{h_{\dot{\delta}}}}{C_{h_{\delta}}}$$

A dot over a symbol represents the time rate of change of the parameter.

THEORETICAL ANALYSIS

A theoretical analysis of the yaw damper is presented to show the parameters that are important in obtaining improved damping. In this analysis the airplane is represented as a single-degree-of-freedom system. This assumption is believed to be satisfactory for determining the changes in period and damping due to a yaw damper actuating the rudder on an airplane of the type used in the present tests. In cases of airplanes with shorter span, high dihedral effect, or other characteristics which increase the importance of the roll-to-yaw coupling, the assumption of a single degree of freedom may not be adequate. In these cases, a more complete theory should be used.

The equation of motion for the airplane is

$$I\ddot{\psi} + \dot{\psi}N_{\dot{\psi}} + \psi N_{\psi} = \delta N_{\delta} \tag{1}$$

The equation of motion for the rudder, if it is assumed to be mass-balanced, is

$$I_r(\ddot{\delta} + \ddot{\psi}) + \dot{\delta}H_{\dot{\delta}} + \delta H_{\delta} = \alpha_t H_{\alpha_t} \tag{2}$$

If sidewash effects are neglected, the angle of attack at the tail α_t is given by the formula

$$\alpha_t = \psi + \frac{l\dot{\psi}}{V} \tag{3}$$

In problems involving motion of a single-degree-of-freedom system, it is convenient to express the dynamic characteristics in terms of the natural frequency ω_n and the damping ratio ζ of the system. Equation (1) may be transformed into

$$\ddot{\psi} + 2\zeta\omega_n\dot{\psi} + \omega_n^2\psi = \delta \frac{N_\delta}{N_\psi} \omega_n^2 \tag{4}$$

where

$$\omega_n = \sqrt{\frac{N_\psi}{I}}$$

$$\zeta = \frac{N_{\dot{\psi}}}{2\sqrt{N_\psi I}}$$

and the term N_δ/N_ψ represents the ratio of sideslip angle to rudder angle in a steady sideslip. It is shown later that the term $I_r(\ddot{\delta} + \ddot{\psi})$ in equation (2) may be neglected for practical values of rudder inertia, hinge moments, and viscous damping. The rudder motion is then represented by the first-order equation

$$\frac{H_{\dot{\delta}}}{H_\delta} \dot{\delta} + \delta = \left(\psi + \frac{l\dot{\psi}}{V}\right) \frac{H_{\alpha_t}}{H_\delta} \tag{5}$$

The term $H_{\dot{\delta}}/H_\delta$ is equal to the time constant τ of the rudder system. The term H_{α_t}/H_δ is the ratio of rudder floating angle to tail angle of

attack with the rudder free. The value of δ may be eliminated between equations (4) and (5) to obtain the characteristic equation of the system

$$D^3 + D^2\omega_n\left(\frac{1}{\tau\omega_n} + 2\zeta\right) + D\omega_n^2\left(1 + \frac{2\zeta}{\tau\omega_n} - \frac{1}{\tau\omega_n}\frac{\omega_n l}{V}\frac{H_{\alpha_t}}{H_\delta}\frac{N_\delta}{N_\psi}\right) + \frac{\omega_n^3}{\tau\omega_n}\left(1 - \frac{H_{\alpha_t}}{H_\delta}\frac{N_\delta}{N_\psi}\right) = 0$$

where $D = \frac{d}{dt}$. This equation shows the primary variables which affect the motion. The variables are, aside from the frequency ω_n and damping ζ of the basic airplane, the quantity $\tau\omega_n$, which is proportional to the ratio of the time constant of the rudder to the period of the uncontrolled airplane oscillation, and the rudder floating parameter $\frac{H_{\alpha_t}}{H_\delta}\frac{N_\delta}{N_\psi}$, which represents the loss in directional stability due to freeing the rudder. When this quantity has a value of 1, the static directional stability with rudder free is 0, as shown by the disappearance of the constant term of the characteristic equation. The only other quantity which appears in the characteristic equation is the ratio $\omega_n l/V$. This quantity occurs in a small term which arises from the effect of yawing velocity on the floating angle of the rudder. This term has only a minor effect on the characteristics of the motion for the limited range of values which it can assume in practice.

The solution of the characteristic equation yields a pair of complex roots representing the lateral oscillation of the airplane as modified by the action of the yaw damper and a real root representing a convergence. The period of the oscillatory mode and the time to damp to one-half amplitude for the convergence may be conveniently expressed in terms of the undamped natural period of the airplane with rudder fixed P_n. These values, together with the number of cycles to damp to one-half amplitude of the oscillatory mode, are shown in figure 2 as functions of the ratio τ/P_n for various values of the rudder floating parameter $\frac{H_{\alpha_t}}{H_\delta}\frac{N_\delta}{N_\psi}$. The calculations were made for $\zeta = 0$ and 0.02 and for $\frac{\omega_n l}{V} = 0.125$. Previous flight data indicated that, at 30,000 feet altitude, ζ was approximately equal to 0.02 for the test airplane.

The calculations show that the lateral oscillation is unstable with $\tau/P_n = 0$ (rudder free and no aerodynamic damping on the rudder) but that the damping rapidly improves with a small amount of viscous restraint or aerodynamic damping on the rudder and reaches a maximum for values of τ/P_n between 0.1 and 0.2. With further increase in the value of τ/P_n, the damping slowly approaches that obtained with the rudder fixed. Calculations indicate that the airplane with rudder fixed has, of course, zero damping for the case of $\zeta = 0$ and damps to one-half amplitude in 5.5 cycles for $\zeta = 0.02$. The value of the real part of the root representing the oscillation was found to be increased negatively by approximately 0.02 for all cases in which ζ was changed from 0 to 0.02. This result indicates that any damping inherent in the airplane with this particular system is added to that contributed by the yaw damper, at least for small values of airplane damping. The optimum damping consistently improves with positive increases in the rudder floating parameter $\frac{H_{\alpha_t}}{H_\delta}\frac{N_\delta}{N_\psi}$, which correspond to increased tendency of the rudder to float with the relative wind. An increase in this quantity, however, represents a loss in static directional stability due to freeing the rudder, as shown by the increase in period of the lateral oscillations with rudder free ($\tau/P_n = 0$). A compromise must, therefore, be made between the conflicting requirements for damping and static stability. It should be noted, however, that, for values of τ/P_n of 0.2 or greater, the period of the oscillations is only slightly greater than that with rudder fixed. This result indicates that, for transient disturbances which are composed mainly of harmonics with periods equal to or less than the period of the lateral oscillations, the viscous restraint for τ/P_n of 0.2 or greater will largely prevent rudder motion in phase with the angle of yaw of the airplane. As a result, rather large decreases in the static directional stability may be tolerable.

For values of τ/P_n and $\frac{H_{\alpha_t}}{H_\delta}\frac{N_\delta}{N_\psi}$ which give rapid damping of the lateral oscillation, the value of the time to damp to one-half amplitude for the aperiodic mode is seen to be short. This mode would not, therefore, be expected to cause any undesirable handling qualities.

In practice, if the aerodynamic parameters are considered to be unaffected by Mach number, the period P_n varies as $1/\sqrt{q}$, whereas the value of τ varies as $1/q$. The quantity τ/P_n, therefore, varies as $1/\sqrt{q}$. (In a hydraulic damper, the value of τ may also vary with temperature unless the damper is compensated for temperature effects.) For this reason, the parameters should be selected to provide adequate damping of the lateral oscillations over a range of values of τ/P_n. The curves of figure 2 indicate, for example, that, for a value of the rudder floating

parameter of 0.5 at $\zeta = 0$, the oscillations will damp to one-half amplitude in less than 1 cycle between the values of τ/P_n of 0.07 and 0.35. The variation of damping with dynamic pressure is determined by the location of the operating range on the curves of figure 2. For example, if a rather large viscous restraint is placed on the rudder, the values of τ/P_n may lie above the minimum point on the curves of $N_{1/2}$ against τ/P_n throughout the speed range. As a result, the damping will increase with increasing dynamic pressure. For smaller values of viscous restraint, on the other hand, the minimum point on the curve may correspond to a low-speed condition, and the damping will decrease with increasing dynamic pressure.

The requirements for improved damping place limitations on the ratios of the rudder hinge-moment parameters $C_{h_{\alpha_t}}$ and C_{h_δ} but no limitations on their magnitudes. Since the value of τ equals $H_\delta^\cdot/H_\delta$, the same value may be obtained with either a large viscous restraint and a large value of C_{h_δ} or a small viscous restraint and a small value of C_{h_δ}. In practice, the minimum value is determined by the need to keep the aerodynamic forces on the rudder sufficiently large compared with the static friction; whereas the maximum value is probably limited by the objectionable effect of excessive viscous restraint on the pilot's ability to move the rudder.

For values of viscous restraint and rudder floating characteristics selected on the basis of the foregoing theory, it is possible to check the effect of rudder moment of inertia which was neglected previously. The importance of rudder moment of inertia is determined by its ratio to the restoring moment H_δ. As noted previously, the value of C_{h_δ} is not uniquely determined by the requirements for improved damping. A reasonable value of C_{h_δ} was, therefore, selected for these calculations, and the other parameters needed were chosen to provide improved damping. The values assumed for rudder characteristics are as follows:

I_r, slug-ft^2	1
b, ft	7.17
c, ft	1.43
C_{h_δ} per degree	-0.003
$C_{h_{\alpha_t}}$ per degree	-0.0015
$H_\delta^\cdot$, ft-lb/radian/sec	304

The values assumed for the flight condition and airplane characteristics are as follows:

q, lb/sq ft	400
P_n, sec	1.5
ζ	0
$\omega_n l/V$	0.125
N_δ/N_ψ	1.0

These conditions were chosen to correspond to the following values of the parameters plotted in figure 2:

τ/P_n	0.2
$\frac{H_{\alpha_t}}{H_\delta}\frac{N_\delta}{N_\psi}$	0.5

A comparison of the calculated characteristics of the motion neglecting and including rudder inertia is given in the following table:

Characteristic	Neglecting rudder inertia	Including rudder inertia
Period, sec	1.68	1.70
Cycles to half amplitude	0.651	0.625
Time to damp to half amplitude	0.334	0.334 0.0023

The rudder motion including inertia is heavily overdamped and results in two modes of convergence. The added mode has such a short-time constant that little effect on the action of the rudder would be expected. The calculations show very little effect on the period and damping of the lateral oscillation. The neglect of rudder inertia is, therefore, believed to be justified in cases of practical interest. The viscous restraint required on the rudder is much greater than the inherent aerodynamic damping of the rudder motion. For this example, the aerodynamic damping on the rudder would be of the order of only 10 ft-lb/radian/sec.

If the value of C_{h_δ} for the rudder was made very small, the importance of rudder inertia would increase. With a very small value of C_{h_δ}, however, the aerodynamic and viscous forces on the rudder would probably be obscured by static friction.

DESCRIPTION OF APPARATUS

The test airplane was a conventional unswept-wing, single-place, two-engine, jet-propelled fighter. All lifting surfaces were the full-cantilever type. Stressed skin construction was used throughout the airplane. The airplane was equipped with trim tabs on all controls. The ammunition cases and one of the 20-millimeter guns were removed to provide space for the required instruments. The maximum gross weight of the test airplane was 16,200 pounds with the center of gravity located at 24.3 percent of the mean aerodynamic chord. A three-view drawing of the airplane and a sketch showing details of the vertical tail are presented in figure 3.

The rudder was not aerodynamically balanced. Mass balance was provided by inset horns, only one of which was exposed to the airstream. The rudder was equipped with a geared tab which also served as a trim tab. The span of the tab was approximately one-third of the rudder span and the tab was mounted at midspan. The linkage ratio of the production tab system was adjustable to 2, 1.4, -1.4, or -2. Since the primary need for improved damping was for the case of small-amplitude oscillations, it was decided that devices which would only function at small angles still might be satisfactory. Therefore, for the purposes of the present investigation, external links were built to provide a gearing of -4 over a small range of rudder angles.

When the tab gearing of -4 to 1 was used, tab stops were provided at $\pm 6^\circ$. A preloaded spring strut was incorporated into the system to permit the rudder to continue to deflect with the tab against a stop. The spring strut, which is shown in figures 4(a) and (b), was preloaded to 54 pounds. The break-out pedal force after the tab reached its stop was then ±12 pounds at zero dynamic pressure. At dynamic pressures corresponding to the flight speed range, some pedal force was required to overcome the aerodynamic hinge moments of the tab with the result that the increment in pedal force that occurred when the tab reached its stop decreased with increasing flight speed. For further deflection of the rudder there was an additional centering force contributed by the spring strut equivalent to 0.65 pound of pedal force per degree of rudder deflection. The breakout moment was designed always to exceed the hinge moment required to hold the tab against a stop so that the tab would always be linked rigidly or held securely against a stop throughout the rudder

deflection range. The preload to hold the tab against the stop was provided as a precaution against flutter since the tab was not mass-balanced.

The rudder control system was primarily a cable-pulley system, but a push-rod connection to the rudder was used in the rear part of the fuselage. The friction of the system was approximately ±2 pounds measured at the pedals. There was approximately ±1/4° play in the rudder system.

For most of the present investigation, the viscous damping cylinder shown in figure 5 was mounted in the tail cone fairing and connected to the base of the rudder torque tube on approximately a 3.5-inch arm. The viscous damping moment provided when 5,000 centistokes fluid was used was 167 ft-lb/radian/sec at 70° F. This moment probably became as high as 400 ft-lb/radian/sec at the effective operating temperatures at 30,000 feet. In order to keep air out of the cylinder, hydraulic lines were run from either end of the cylinder through a T-shaped joint to an accumulator. The lines and accumulator contained damping fluid subjected to air pressure of 100 lb/sq in. The damping obtained was from two sources. Viscous shear resulting from the piston movement in the cylinder and fluid flow through the cylinder plumbing caused a part of the restraint. The major portion of the damping was from two restricting nozzles in the T-shaped section of the cylinder plumbing.

Modifications which were made to the rudder and tab to vary the hinge-moment parameters are shown in figure 6. These modifications consisted of three sets of trailing-edge strips which were used on the portion of the rudder trailing edge not covered by the tab and a 22° beveled balancing tab which was built up from a production tab. This modified tab was used in conjunction with the triangular trailing-edge strips.

In order to be able to measure the damping of the lateral oscillations with the rudder fixed, a rudder-locking mechanism which was controllable from the cockpit was installed. The arresting hook control system of the airplane was connected to a large spring-loaded taper pin which was mounted, with a socket provided, at the base of the rudder. (See fig. 5(a).) Even with the pin engaged, approximately ±1/4° of rudder play was present.

INSTRUMENTATION

Standard NACA recording instruments were installed and used to measure indicated airspeed, pressure altitude, control positions, control forces, sideslip angle, angle of attack, heading, angular velocities, angular accelerations, and normal, transverse, and longitudinal accelerations. These quantities were measured with respect to the body axes of the airplane. The altitude and airspeed measurements were made with

a high-speed pitot-static tube mounted approximately 1 chord length ahead of and slightly below the right wing tip. The recording sideslip vane and angle-of-attack vane were mounted on a boom approximately 1 maximum fuselage diameter ahead of the nose. In order to measure small angles accurately, the sensitivity of both the rudder-position recorder and the sideslip recorder was set at approximately 10° per inch of film deflection. The accuracy of measured increments of β and δ was then approximately $\pm 0.1^{\circ}$

TESTS

Lateral oscillations were performed by releasing the controls in steady sideslips. If the oscillation was to be made rudder-fixed, the rudder lockpin was set to engage the first time the rudder passed through neutral. In order to determine hinge-moment parameters, step-input rudder kicks were made in the various test configurations with the damping cylinder disengaged. It is possible to determine the rate of change of hinge-moment coefficient with rudder deflection from the initial portion of the maneuvers in which the sideslip is essentially constant. The rate of change of hinge-moment coefficient with angle of sideslip, which is an approximate measure of the rate of change of hinge moment with angle of attack of the vertical tail, can be evaluated from the control-fixed portion of the maneuver in which the angle of sideslip builds up. Steady sideslips were made to determine the effect of the various rudder modifications on the static directional stability and to indicate whether the airplane was properly trimmed. In most cases, test runs were made at 10,000 feet at speeds from 200 to 330 knots and at 30,000 feet at speeds from 200 to 300 knots. The corresponding Mach number range was from 0.35 to 0.71 at 10,000 feet and from 0.55 to 0.75 at 30,000 feet.

Simulated strafing runs were made to determine how well the airplane with modified rudder configuration could be held on a fixed target. A rough-air flight was made in which the final damper configuration was used with the rudder locked and unlocked on alternate runs. The results were inconclusive, partly because of play in the locking mechanism and partly because of the small magnitude of turbulence encountered.

RESULTS AND DISCUSSION

Original Configuration

As shown in figure 7, the measured rudder-free lateral damping characteristics of the test airplane were unsatisfactory according to the requirements of reference 4 at 10,000 feet and were more unsatisfactory at 30,000 feet. These data have been previously presented and discussed in reference 5.

The measured damping of the test airplane with rudder fixed is also presented in figure 7. Comparison of the data in this figure shows that, for the production configuration of the rudder control system, the damping of the lateral oscillation deteriorated noticeably when the rudder was freed. Figures 8 to 10, obtained from reference 5, present the variation of hinge-moment coefficient with rudder deflection and angle of sideslip and a time history of a rudder-free lateral oscillation.

For the unmodified or production configuration, which was equipped with a 1.4-to-1 unbalancing tab and had no aerodynamic balance, the restoring moment parameter C_{h_δ} was large and relatively linear with a value of approximately -0.011 per degree. The variation of hinge-moment coefficient with angle of sideslip was nonlinear and at small angles of sideslip the value of the floating moment parameter $C_{h_{\alpha_t}}$ was approximately 0.0013. During controls-free lateral oscillations, the rudder lagged behind the angle of sideslip by as much as 20°, that is, 1/18 cycle, and appeared to be feeding an appreciable amount of energy into the oscillation.

First Modification

The simplified analysis presented previously indicated that a negative value of $C_{h_{\alpha_t}}$ of approximately -0.0015 per degree and a reduction of C_{h_δ} to one-third or one-fifth of its initial value when used in conjunction with viscous damping of 100 to 200 ft-lb/radian/sec would provide appreciable improvement of the controls-free lateral oscillation. In order to adjust the hinge-moment parameters for improved damping, 1/8-inch-square trailing-edge strips were installed inboard and outboard of the tab (to make $C_{h_{\alpha_t}}$ more negative) and the tab was changed from an unbalancing tab to a balancing tab with a linkage ratio of -2 to counteract the increased negative C_{h_δ} caused by the strips and, in addition, to reduce C_{h_δ} further. (See table I.)

The approximate hinge-moment variations with deflection and sideslip angle as determined for this configuration from rudder kicks are presented in figures 11 and 12. Figure 13 is a time history of a lateral oscillation for the modified configuration. The variation of time to damp to one-half amplitude against period for the modified configuration with the damper and also without the damper is shown in figure 7. It should be noted that even without the use of the damping cylinder a considerable improvement in the damping of the lateral oscillation had been effected. The pour point of the damping fluid used in the damping cylinder is approximately -50° C. Free-air temperatures encountered during the flight tests at 30,000 feet altitude were of the order of -35° C. The viscosity increase as a result of the low temperature caused the rudder to be overdamped at large deflections and to have a tendency to stick at the small amplitudes. A comparison of the damped and undamped configuration is presented in figure 7.

In many cases the beneficial effects of such modifications could be easily investigated on prototype airplanes which are found to have unsatisfactory damping of lateral oscillations.

Second Modification

Although the damping of the lateral oscillation was measurably improved by use of a damping cylinder in conjunction with the first modifications, it was apparent that further improvement in the damping from further adjustment of the hinge-moment parameters would be desirable. Therefore, the trailing-edge strips were enlarged and the tab gearing was increased to -4 over a limited range of deflections. Table I shows the approximate measured or estimated hinge-moment parameters which apply at small angles for the various configurations which have been considered. For the second modification, $C_{h_{\alpha_t}}$ was estimated and C_{h_δ} was calculated from steady sideslip data of figure 14 by using the estimated value of $C_{h_{\alpha_t}}$.

Time histories obtained at altitudes of 10,000 and 30,000 feet of the damping of the controls-free lateral oscillation with the 1/4-inch trailing-edge strips and the tab gearing of -4 to 1 are presented in figure 15. Comparison of these data for 10,000 feet with the time history for the production configuration presented in figure 10 demonstrates the marked improvement in damping obtained. However, the time history obtained at 30,000 feet indicates that further increase in damping would be desirable. Figure 16 shows that the time to damp to one-half amplitude was decreased appreciably by the second modification. For the test airplane, the damping was made to satisfy approximately the flying-qualities requirement.

On one flight, damping data were obtained with the viscosity of the damping fluid reduced approximately 50 percent. The effect on the measured damping was small.

Proper trimming of the rudder within the small travel in which the tab was geared was critical with the test installation. The usable tab travel at the gearing of -4 to 1 was limited by the mechanical strength of the spring in the spring strut. At a dynamic pressure corresponding to 330 knots at 10,000 feet, the yield strength of the spring permitted use of a preload sufficient to counteract the estimated hinge moments for ±6° tab deflection. For a tab gearing of -4 to 1 or slightly more, the rudder travel in the low C_{h_δ} range was less than ±1.5°.

In order to obtain maximum benefit from the damping device, it was necessary that the airplane be trimmed with the tab in the center of its operating range. Proper trim was established by small cut-and-try preflight tab adjustments and by the use of eccentric trailing-edge strips on the rudder. These results lead to the conclusion that, although damping is required only for small deviations from the trim condition, a larger linear operating range for a damper of this type is required than was provided in the test installation. The increased operating range is required to allow for lateral trim changes of the airplane.

Third Modification

An additional configuration has been tested on which modifications shown in figure 6 were made to the tab section and trailing-edge strips in an attempt to increase further the ratio of $C_{h_{\alpha_t}}$ to C_{h_δ}. The rectangular strips were replaced with triangular strips which were blunt at the rear and projected further, 7/16 inch on the left surface and 3/8 inch on the right, in an attempt to make $-C_{h_{\alpha_t}}$ more negative. In order to reduce the appreciable hinge moments per degree of rudder travel required to deflect the highly geared tab, the tab was beveled over the rear 25 percent of its chord. The modified trailing-edge angle was approximately 22°.

Some further improvement in the damping of the controls-free lateral oscillation resulted as indicated by test runs for which times to damp to one-half amplitude are presented in figure 16. A time history that shows the improved damping at 10,000 feet and 300 knots is presented in figure 17. With the beveled tab, a reduction in hinge moment was evidenced by the fact that the rudder tended to float to larger angles. As a result, the tab hit both stops during the initial cycle of some oscillations.

The hinge-moment parameters for this configuration were determined from step-input rudder kicks and steady sideslips. Figure 18 presents

the measured variation of rudder hinge-moment coefficient with angle of sideslip obtained from the rudder kicks. Figure 19 presents the variation of rudder control force and rudder position with angle of sideslip. A further reduction in the ratio $C_{h_\delta}/C_{h_{\alpha_t}}$ resulted from use of the triangular strips as can be seen from table I which summarizes the hinge-moment parameters for all configurations tested.

Figure 19 shows an example of the steady sideslip characteristics of the test airplane with the tab geared only for a small range of deflections. The pedal-force gradient at small deflections was a small fraction of the gradient at larger deflections. The flying qualities of the test airplane with this pedal-force characteristic were considered to be unsatisfactory. This characteristic was noticed by the pilot whenever small heading corrections were required such as during a simulated strafing run.

A measure of the effectiveness of a damping augmenter would be that the damper should make it possible to hold the airplane more closely on a target with the amplitude of oscillation about the target reduced and the damping increased. Simulated strafing runs indicated that the nonlinear pedal-force gradient with very light forces for small deflections hindered the pilot's ability to hold the airplane closely on a target or to phase properly the control motion to supplement the inherent damping of the configuration.

Another consequence of the small values of $C_{h_{\alpha_t}}$ and C_{h_δ} existing on the test installation for small rudder deflections was the relatively small aerodynamic hinge moments available to move the rudder during its action as a yaw damper. It is estimated that, for the third modification, a pedal force of 15 pounds would have been required to hold the rudder fixed at a sideslip angle of 1° at 350 knots. Although the aerodynamic hinge moments were sufficiently large to overcome static friction in the system with rudder free down to very small amplitudes of oscillation, the pressure of the pilot's feet on the rudder pedals largely prevented the yaw damper action in normal flight.

A likely method of eliminating these undesirable characteristics on a practical application of the damping augmenter would be to make use of a wider chord rudder. By increasing the ratio of rudder chord to vertical-tail chord, it is possible to make $C_{h_{\alpha_t}}$ more negative and to increase the ratio of $C_{h_{\alpha_t}}$ to C_{h_δ}, in which case the ratio of $C_{h_{\alpha_t}}$ to C_{h_δ} dictated by the damping requirements can be obtained without requiring that the restoring tendency C_{h_δ} be made so small. In that event, it would no longer be necessary to use balancing devices which produce nonlinear force gradients. Also, with larger rudder hinge moments involved, there would be more tendency for the damper to function effectively with

the pilot's feet on the rudder pedals. In addition, the minimum amplitude at which the damping augmenter would function, which is dependent on the amount of friction in the rudder system and the damper, would be further decreased.

The measured damping of the various test configurations is summarized on one plot of log decrement as a function of Mach number in figure 20. A summary plot of $T_{1/2}$ against P for the various configurations has been presented in figure 16. The data of figure 20 indicate that the effectiveness of the damping device is decreasing appreciably at Mach numbers above 0.7.

CONCLUDING REMARKS

From a flight investigation at Mach numbers up to 0.8, it was possible to achieve considerable improvement in the damping of the rudder-free lateral oscillations of the test airplane by adjusting the pertinent parameters in the manner indicated by the simplified theory. The flight data obtained were in good fundamental agreement with the calculated values of the theoretical analysis. The number of cycles to damp to one-half amplitude which had been 2 to 3 was reduced to 0.5 to 1.5. This degree of improvement was sufficient to make the test airplane approximately satisfy the current criterion for satisfactory lateral damping. However, the adjustment of the rudder floating moment parameter $C_{h_{\alpha_t}}$ to sufficiently large negative values by the use of trailing-edge strips was not practical with the rudder configuration of the test airplane. Therefore, it was necessary to balance closely the rudder restoring tendency C_{h_δ} in order to obtain a favorable ratio of $C_{h_{\alpha_t}}$ to C_{h_δ} close to unity. This procedure was made more difficult by the fact that the trailing-edge strips caused large increases in C_{h_δ}. Adjusting C_{h_δ} to the necessary extent with a balancing tab also tended to be impractical because of the large tab-to-rudder-deflection ratio required. This difficulty occurred because a highly deflected tab appreciably reduced rudder effectiveness and because the rudder hinge moment required to deflect the tab increases with the square of the tab deflection ratio.

The ratio of $C_{h_{\alpha_t}}$ to C_{h_δ} depends on the ratio of the rudder chord to the chord of the vertical tail. It appears likely that a more suitable method of obtaining a larger ratio of $C_{h_{\alpha_t}}$ to C_{h_δ} would be to increase the chord ratio. Since the rudder forces increase as the square of the

chord ratio, aerodynamic balancing, which was not used on the unmodified test airplane, might be required. A small amount of overhanging balance could be used with no large adverse effect on the value of $C_{h_{\alpha_t}}$. This means could be supplemented by the use of a balancing tab. In this event, more moderate tab-linkage ratios should be adequate.

Although the results presented herein indicate that the damping of the lateral oscillation was increased at Mach numbers up to 0.8 by the damping augmenter, it is not certain that the device would be suitable for application to airplanes which operate over a greater speed range, because of the large changes in hinge-moment parameters which usually occur at transonic speeds.

Langley Aeronautical Laboratory,
National Advisory Committee for Aeronautics,
Langley Field, Va., March 25, 1954.

REFERENCES

1. Stough, Carl J., and Kauffman, William M.: A Flight Investigation and Analysis of the Lateral-Oscillation Characteristics of an Airplane. NACA TN 2195, 1950.

2. Greenberg, Harry, and Sternfield, Leonard: A Theoretical Investigation of the Lateral Oscillations of an Airplane With Free Rudder With Special Reference to the Effect of Friction. NACA Rep. 762, 1943. (Supersedes NACA ARR, Mar. 1943.)

3. Schueller, Carl F., Korycinski, Peter F., and Strass, H. Kurt: Tests of a Full-Scale Horizontal Tail Surface in the Langley 16-Foot High-Speed Tunnel. NACA TN 1074, 1946.

4. Anon.: Specification for Flying Qualities of Piloted Airplanes. NAVAER SR-119B, Bur. Aero., June 1, 1948.

5. Crane, H. L., Beckhardt, A. R., and Matheny, C. E.: Flight Measurements of the Lateral Stability and Control Characteristics of a High-Speed Fighter Airplane. NACA RM L52B14, 1952.

TABLE I

RUDDER HINGE-MOMENT PARAMETERS FOR CONFIGURATIONS TESTED

Configuration			Parameters		
Tab-linkage ratio	Trailing-edge strips, in.	Viscosity of damping fluid, centistokes at 70° F	$C_{h_{\alpha_t}}$ per degree	C_{h_δ} per degree	$H_{\dot{\delta}}$ ft-lb/radian/sec at 70° F
1.4	None	0	0.0013	-0.011	0
-2	Square: 1/8 by 1/8	0	-.001	-.005	0
		5,000	-.001	-.005	-167
-4	Square: 5/16 by 1/4 (left side), 1/4 by 1/4 (right side)	5,000	Estimated, -.0015	-.0014	-167
-4	Triangular: 7/16-inch leg (left side), 3/8-inch leg (right side)	5,000	-.0026	-.0016	-167

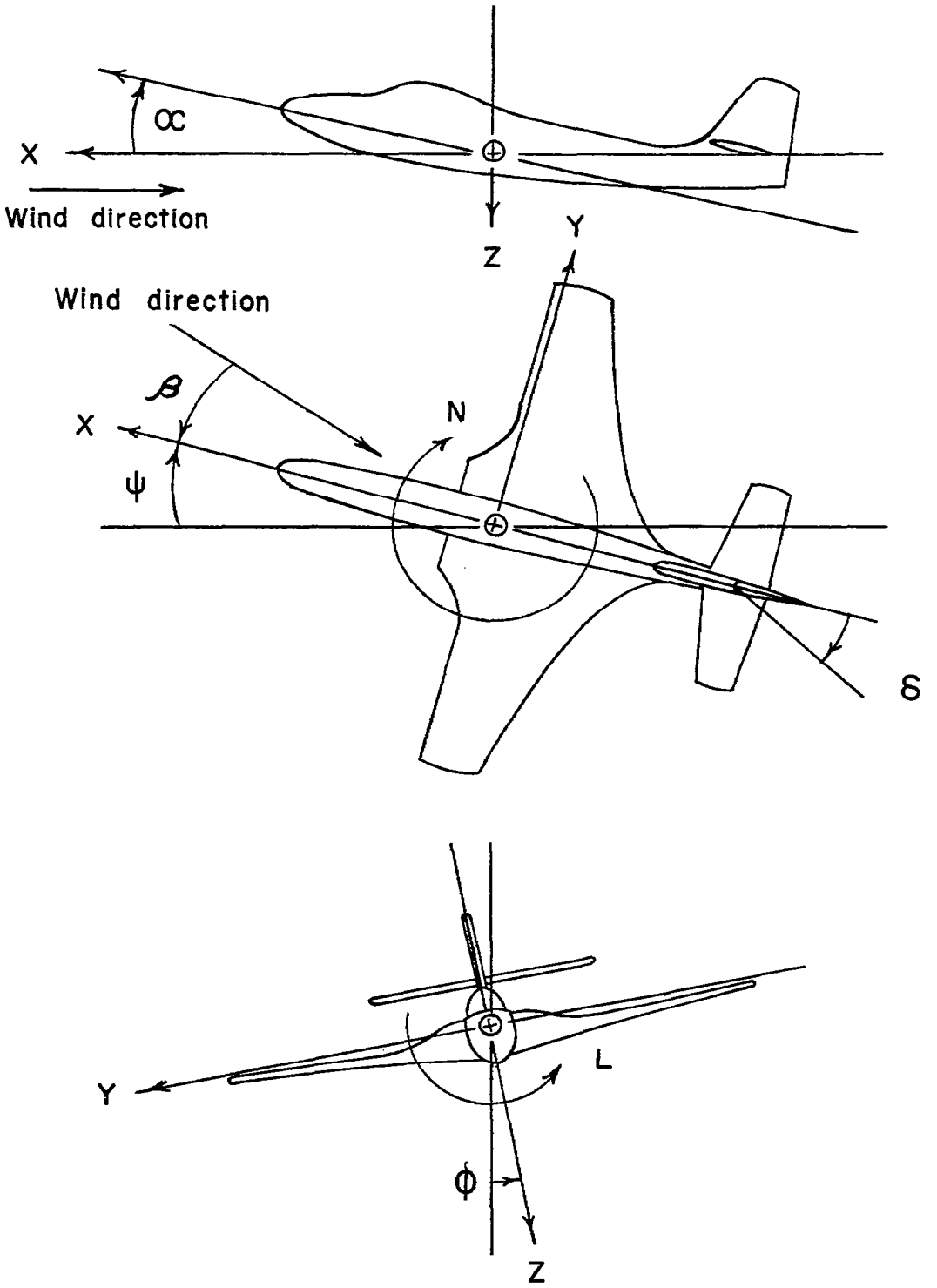

Figure 1.- Stability system of axes. Arrows indicate positive directions of moments, forces, and angles.

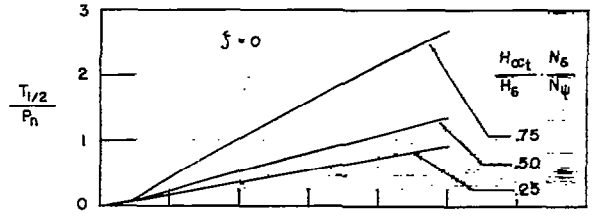

(a) Value of $\frac{T_{1/2}}{P_n}$ for convergent mode as function of τ/P_n. (Values are nearly the same for $\zeta = 0$ and $\zeta = 0.02$.)

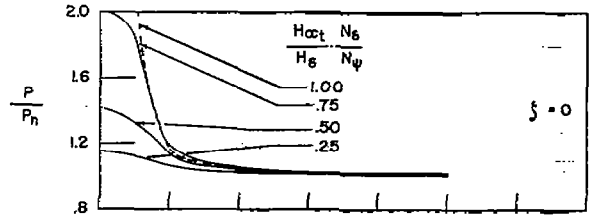

(b) Value of P/P_n of oscillatory mode as function of τ/P_n. (Values are nearly the same for $\zeta = 0$ and $\zeta = 0.02$.)

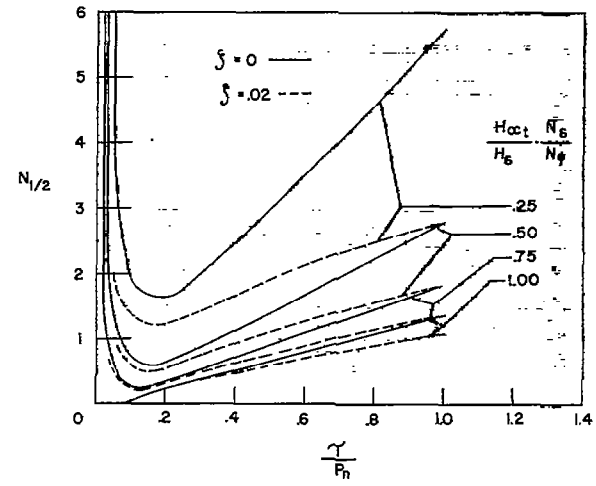

(c) Value of $N_{1/2}$ of oscillatory mode as function of τ/P_n, and for values of $\zeta = 0$ and $\zeta = 0.02$.

Figure 2.- Theoretical effects of yaw damper on characteristics of lateral motion for several values of the parameter $\frac{H_{\alpha t}}{H_\delta}\frac{N_\delta}{N_\psi}$.

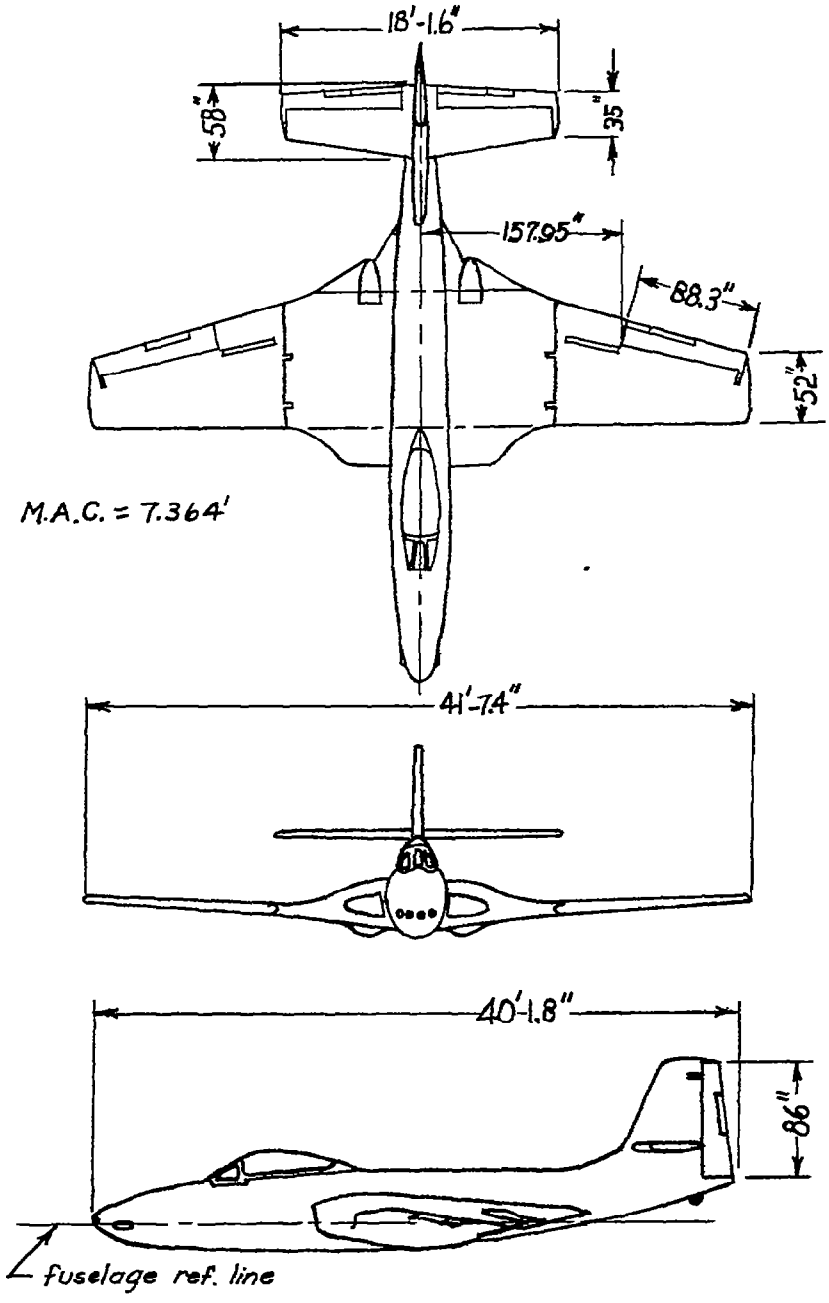

(a) Three-view drawing.

Figure 3.- The test airplane.

Vertical-tail specifications

Tail length, ft	empty	17.28
	full	17.17
Area, sq ft		38.36
Span, ft		7.17
Aspect ratio		1.34
Section	NACA 65(10)-011	
Rudder area, sq ft		10.13
Rudder span, ft		7.17
Rudder root-mean-square chord, ft		1.43

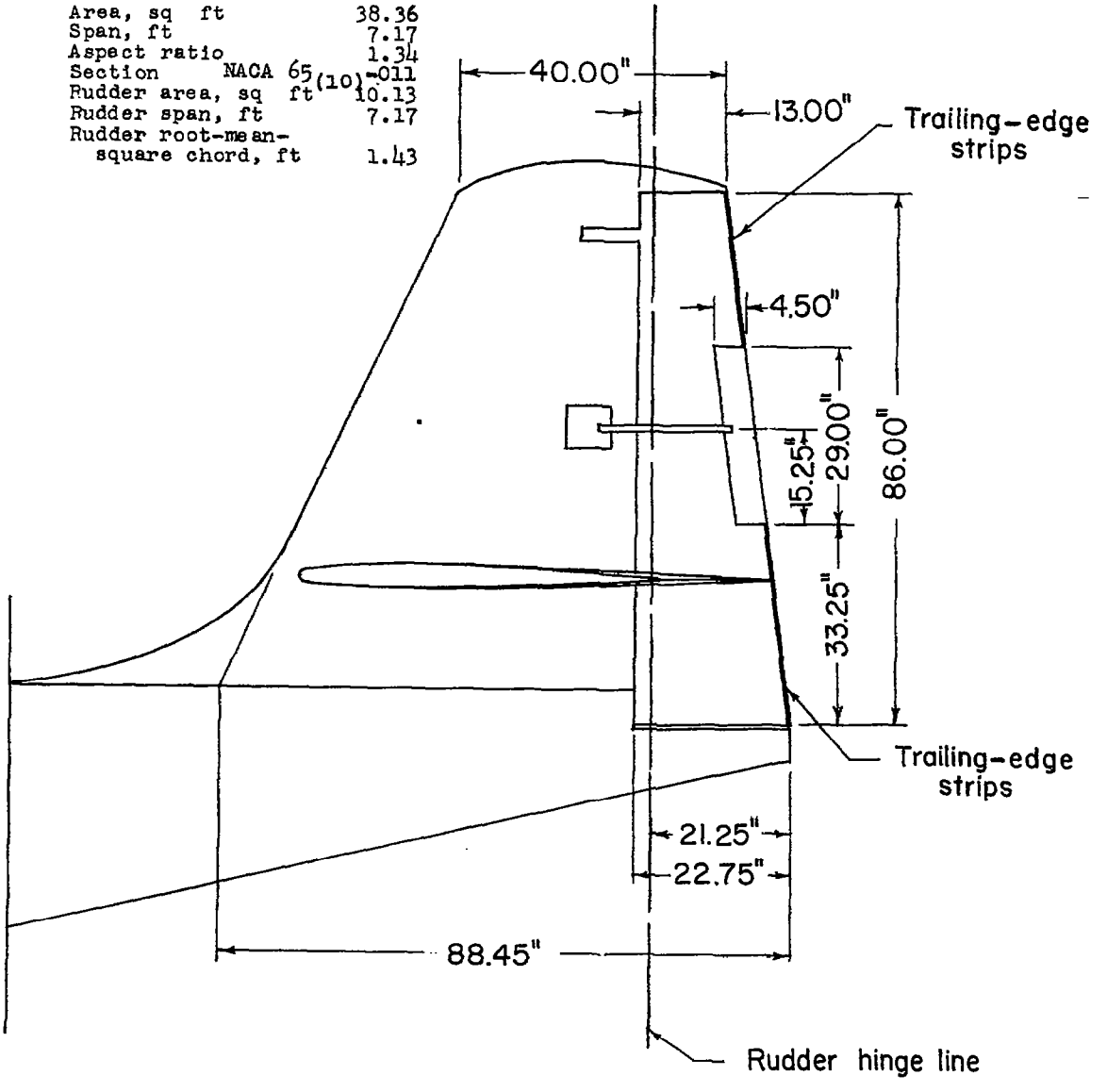

(b) Vertical tail.

Figure 3.- Concluded.

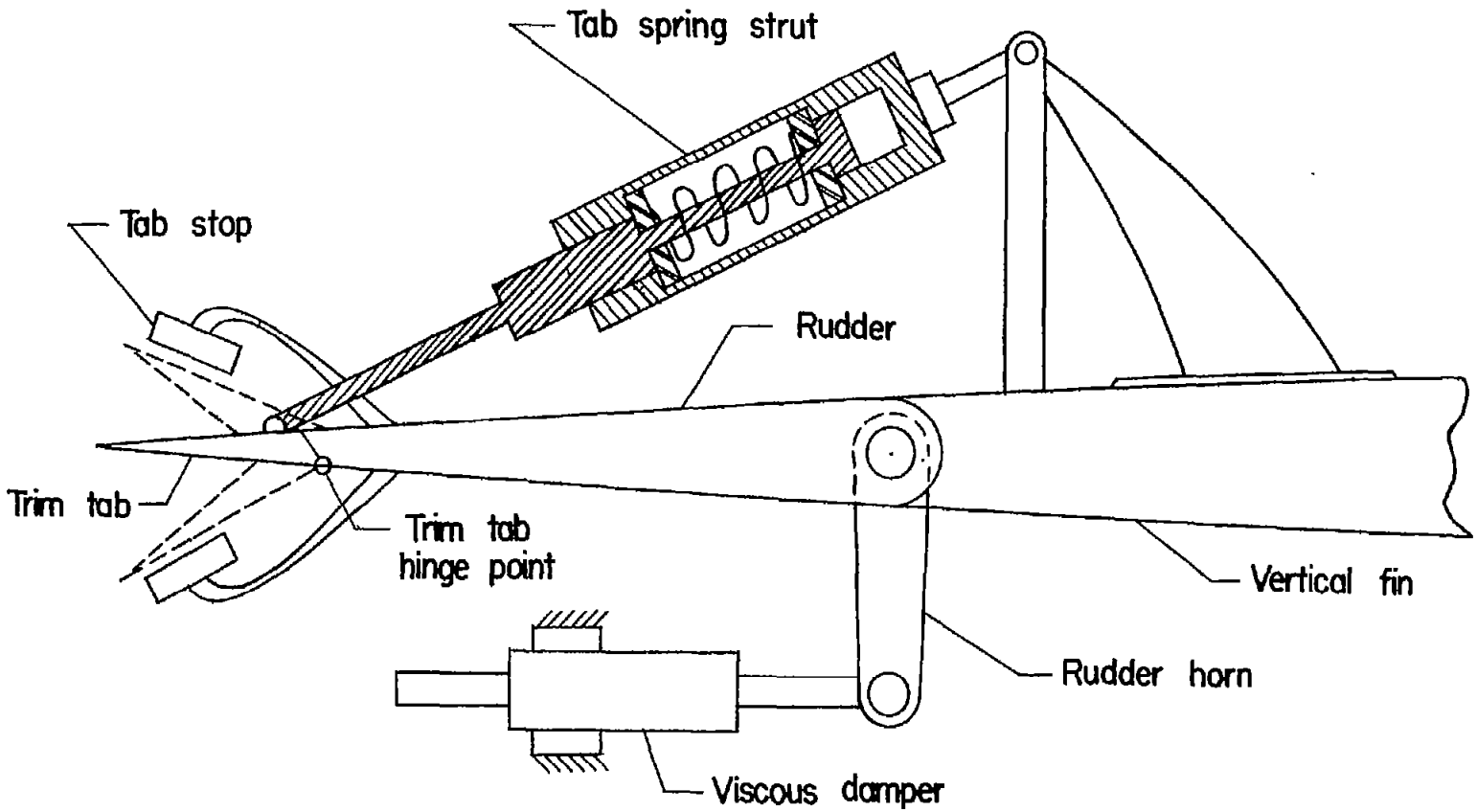

(a) Schematic section view.

Figure 4.- Rudder-tail spring strut.

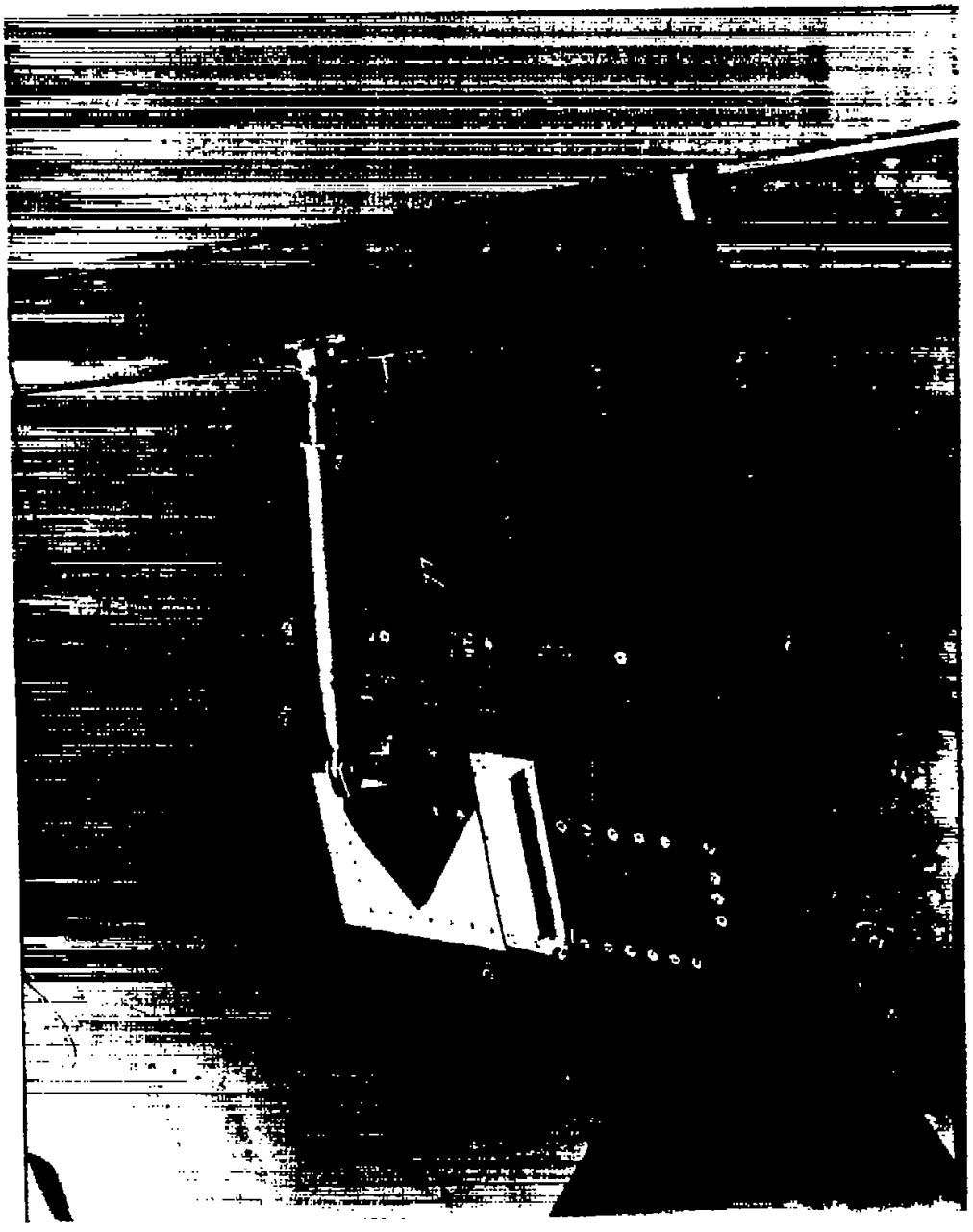

L-80042

(b) Photograph of spring strut and tab.

Figure 4.- Concluded.

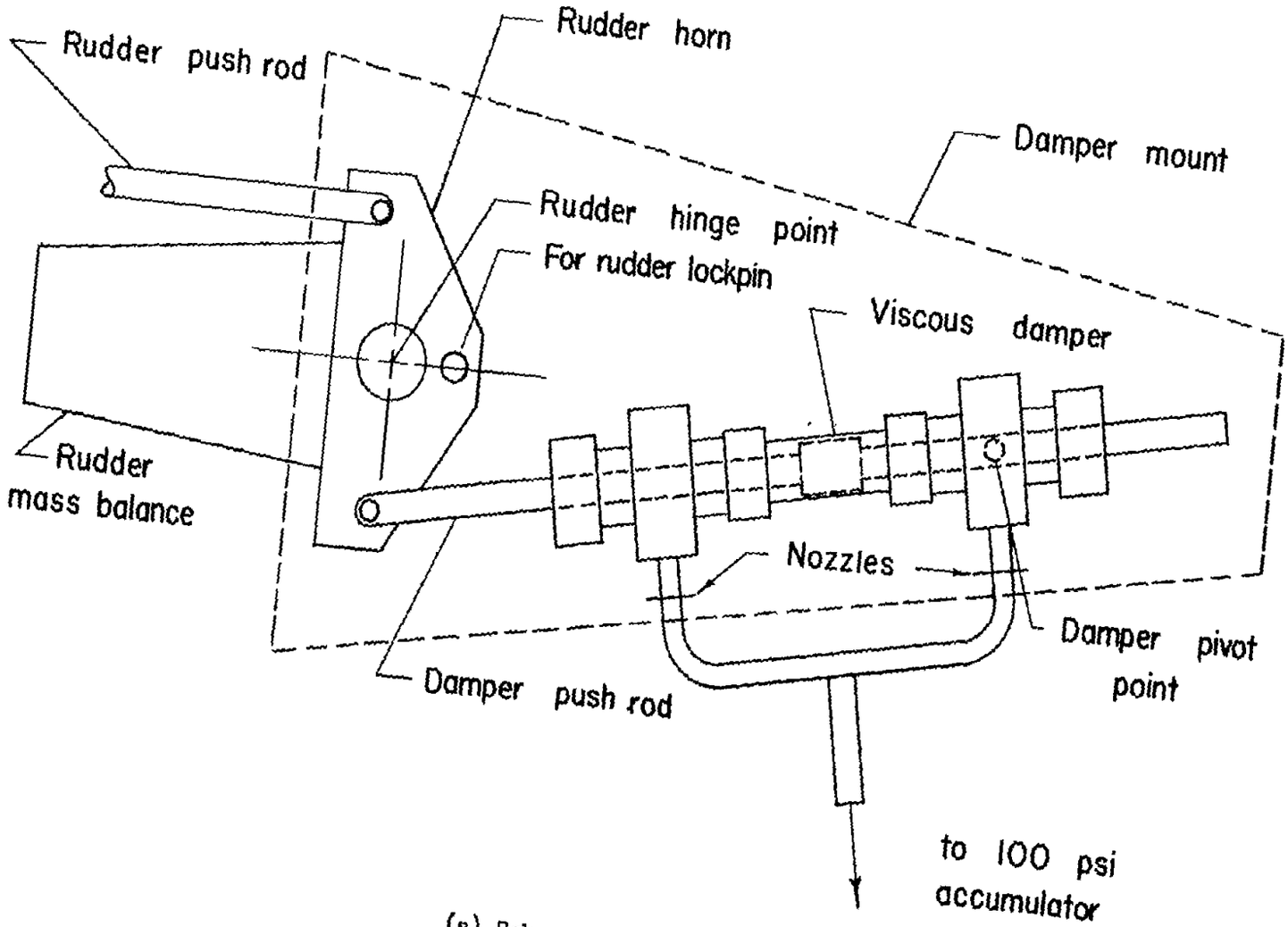

(a) Schematic drawing.

Figure 5.- Viscous damper assembly.

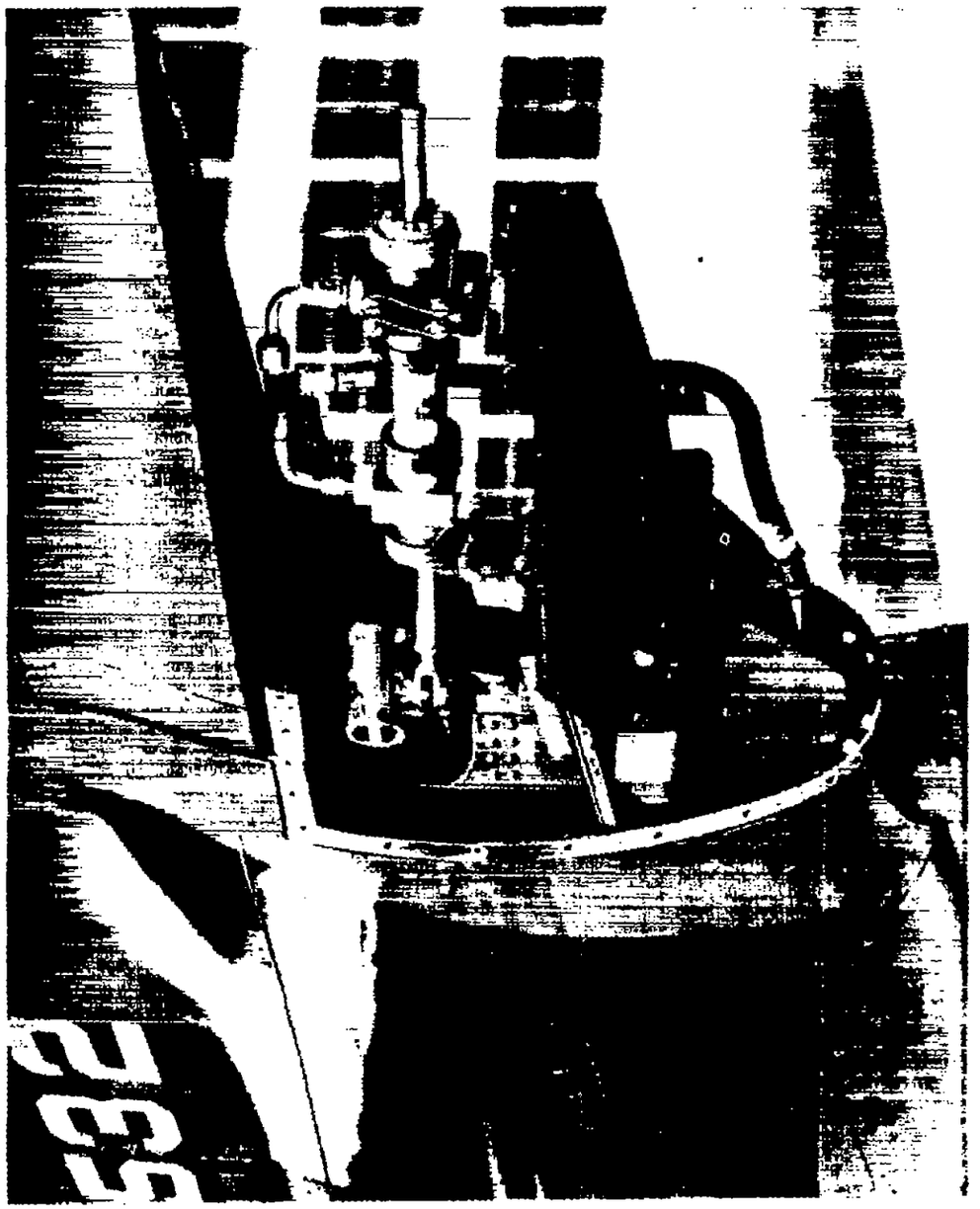

L-80043

(b) Closeup photograph.

Figure 5.- Continued.

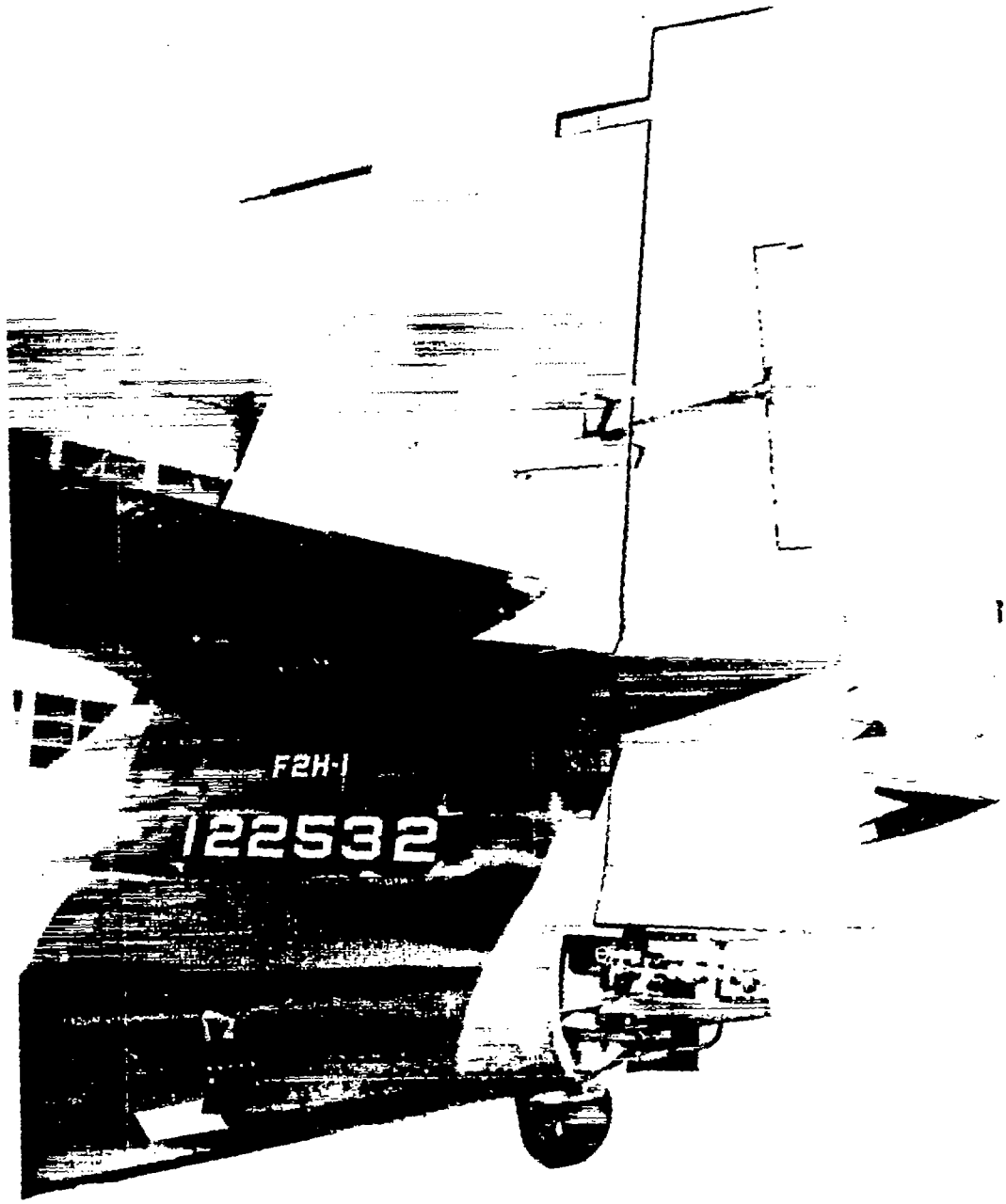

L-80044

(c) Photograph showing tail group of test airplane.

Figure 5.- Concluded.

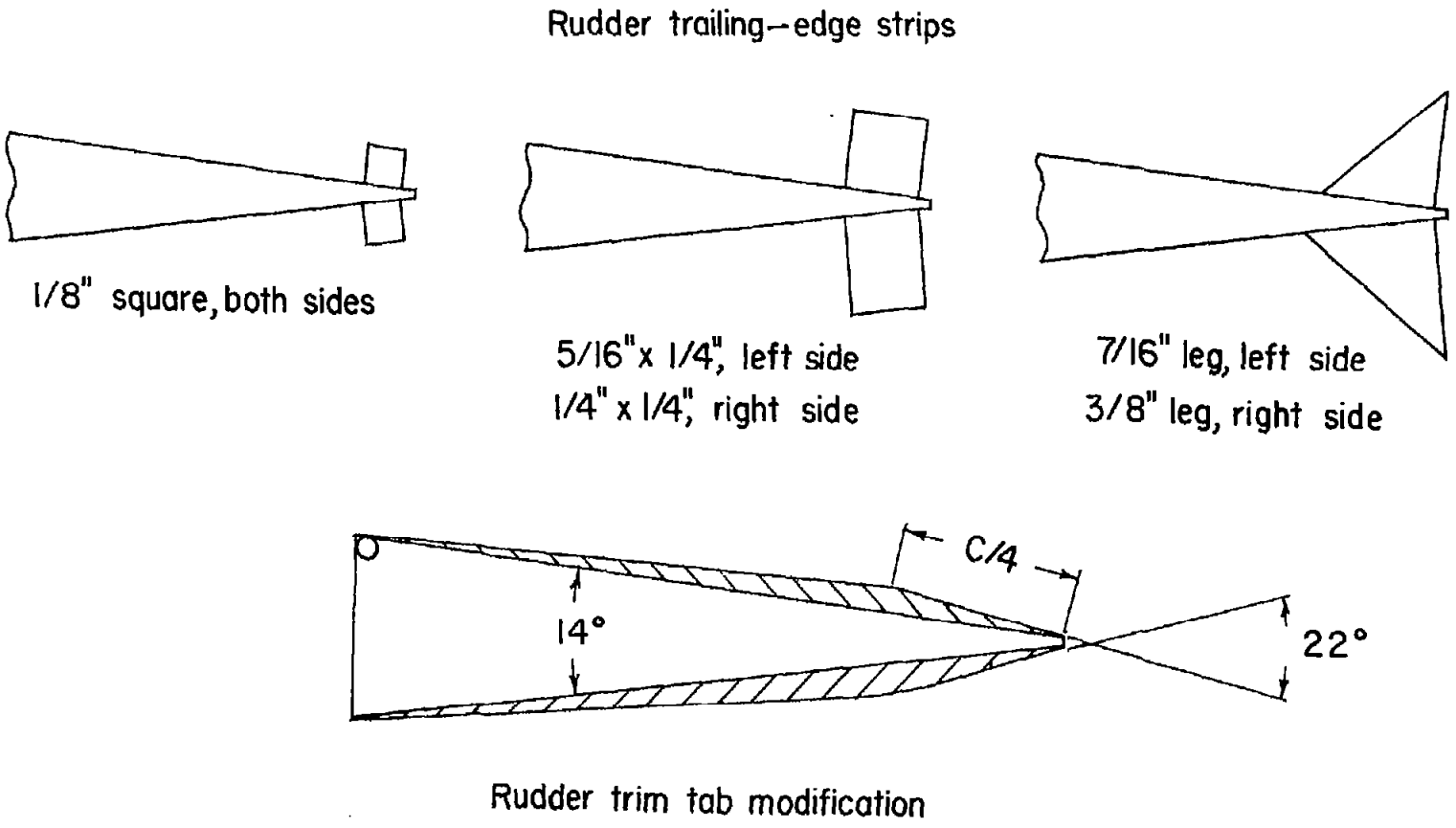

Figure 6.- Sketch showing types of rudder trailing-edge strips tested and rudder trim tab modification.

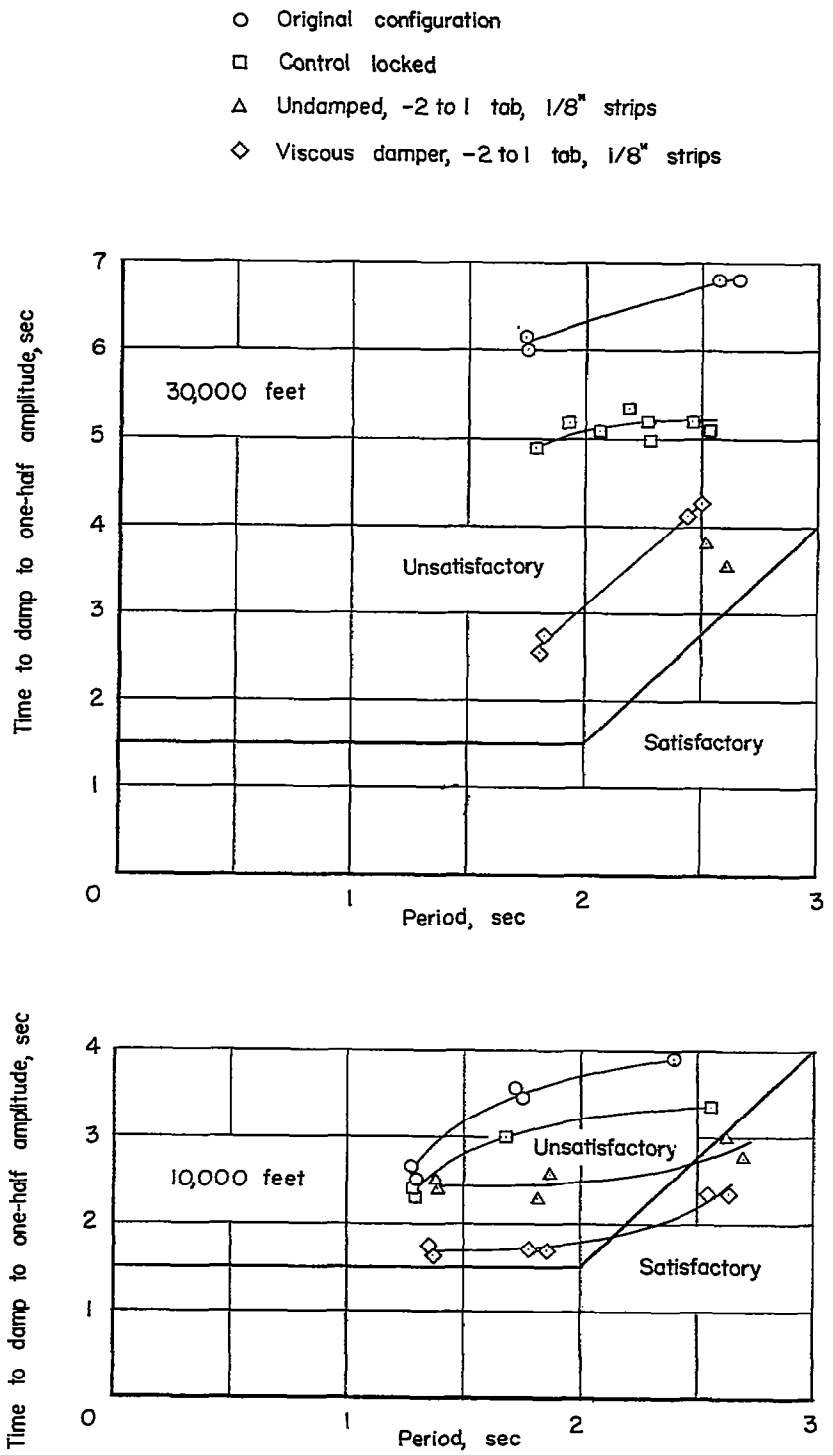

Figure 7.- Measured damping of lateral oscillation. Original configuration and first modification. Viscous damper, 167 ft-lb/radian at 70° F. The boundary between satisfactory and unsatisfactory regions is that specified by the requirements of reference 4.

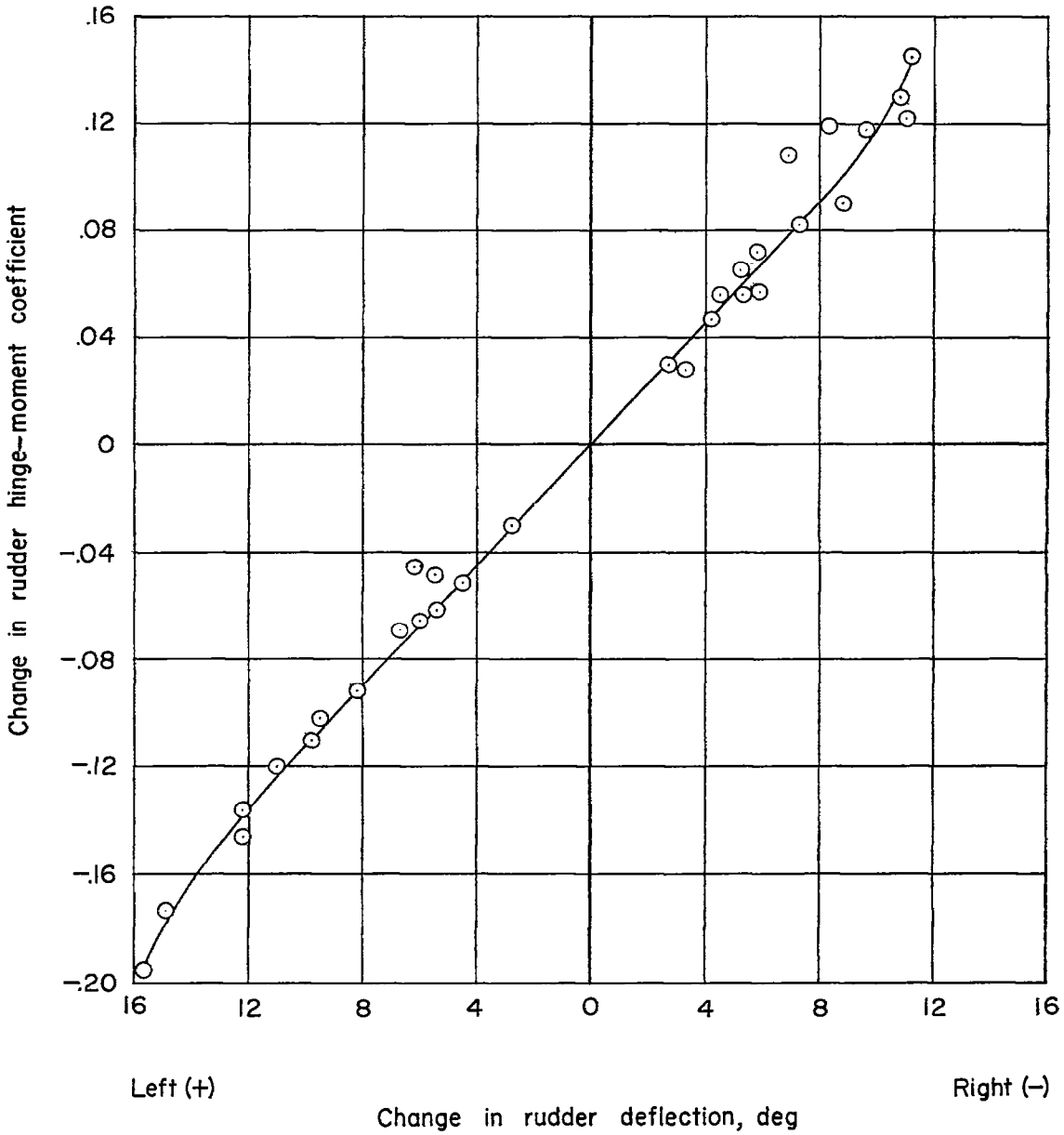

Figure 8.- Change in rudder hinge moment due to change in rudder deflection. Original configuration. Altitude, 10,000 and 30,000 feet; unbalancing tab ratio, 1.4:1.

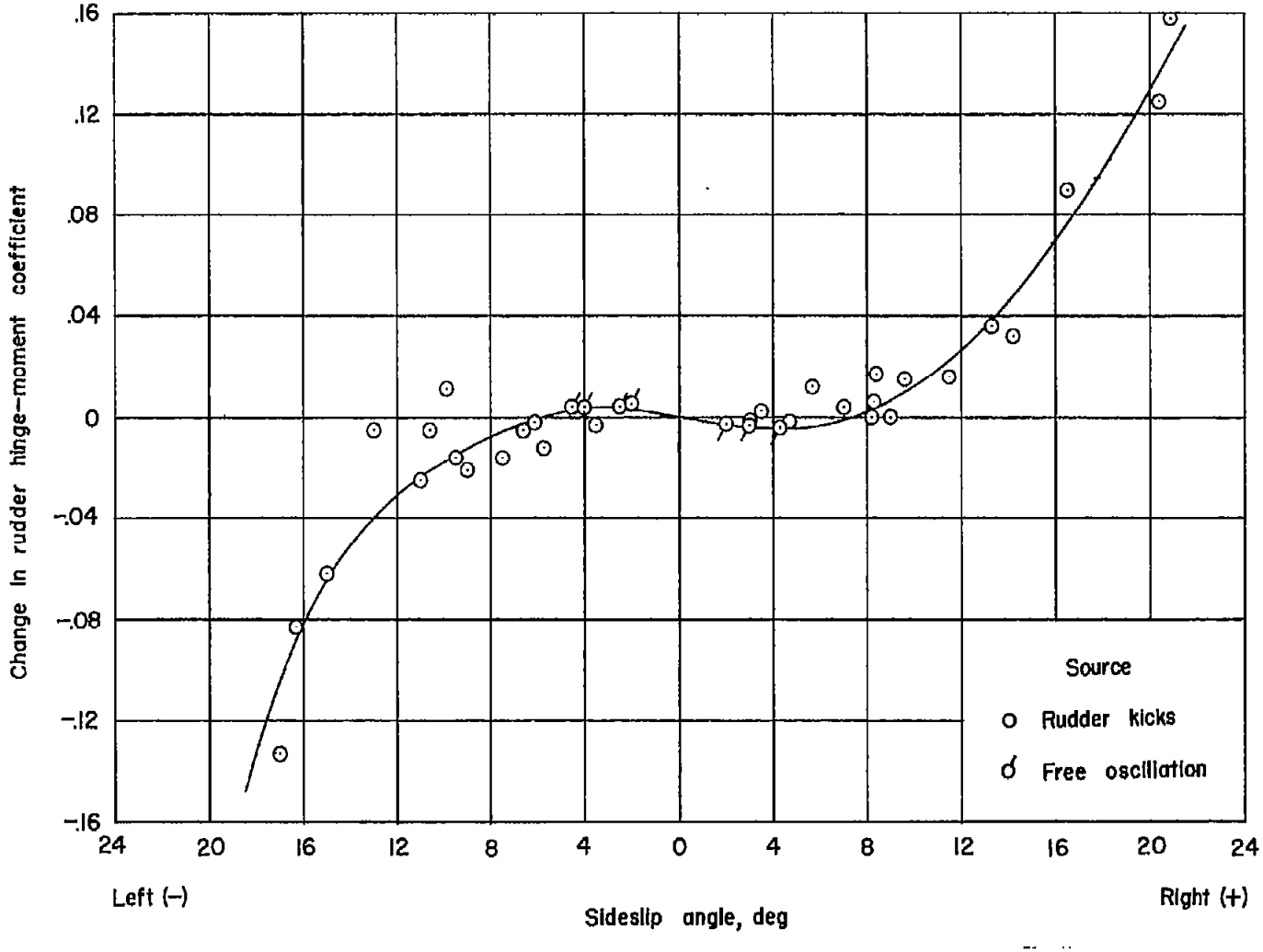

Figure 9.- Change in rudder hinge moment due to sideslip angle. Original configuration. Altitude, 10,000 and 30,000 feet; unbalancing tab ratio, 1.4:1.

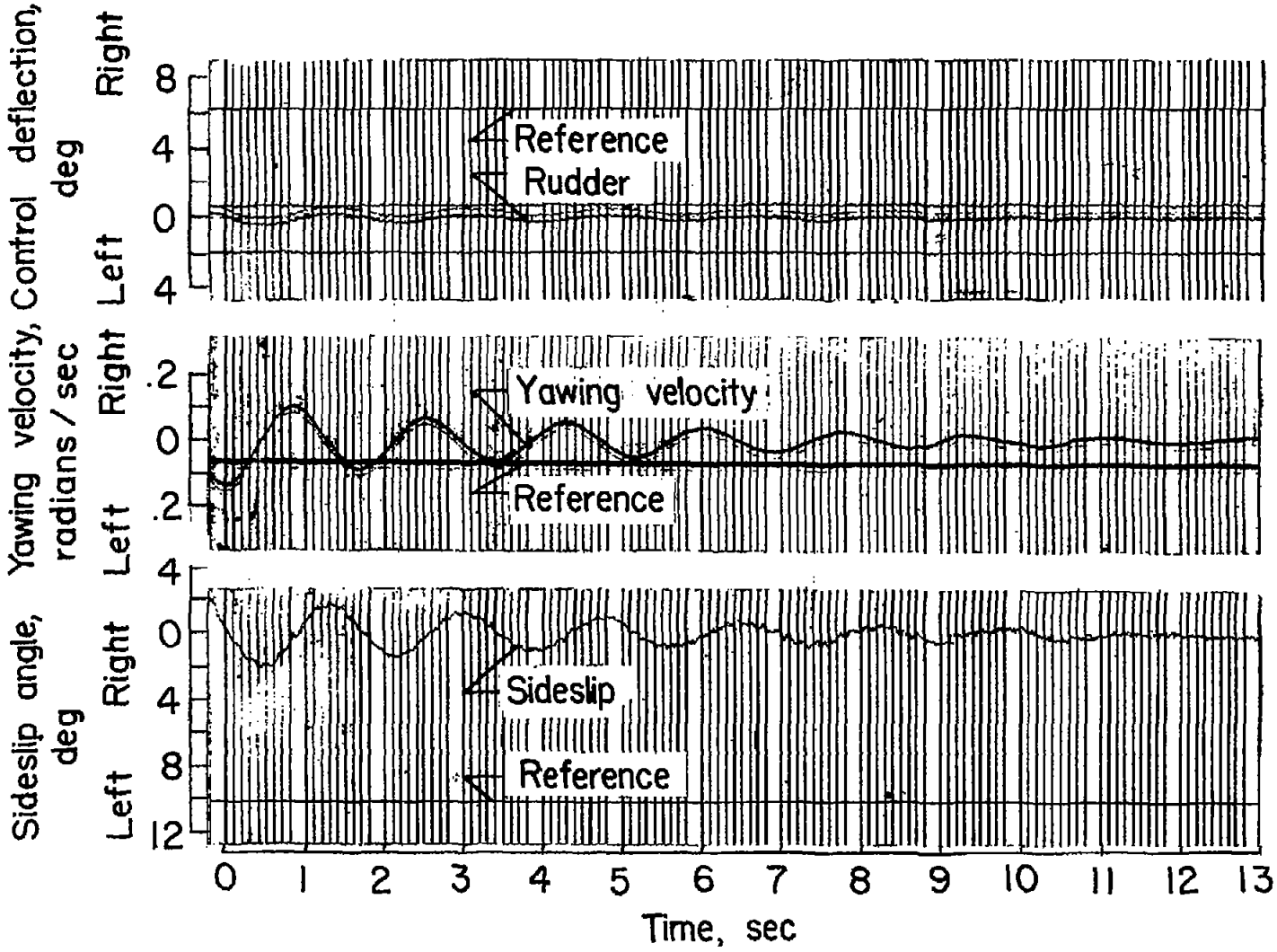

Figure 10.- Time history of rudder-free lateral oscillation. Original configuration. M = 0.53; h_p = 10,000 feet.

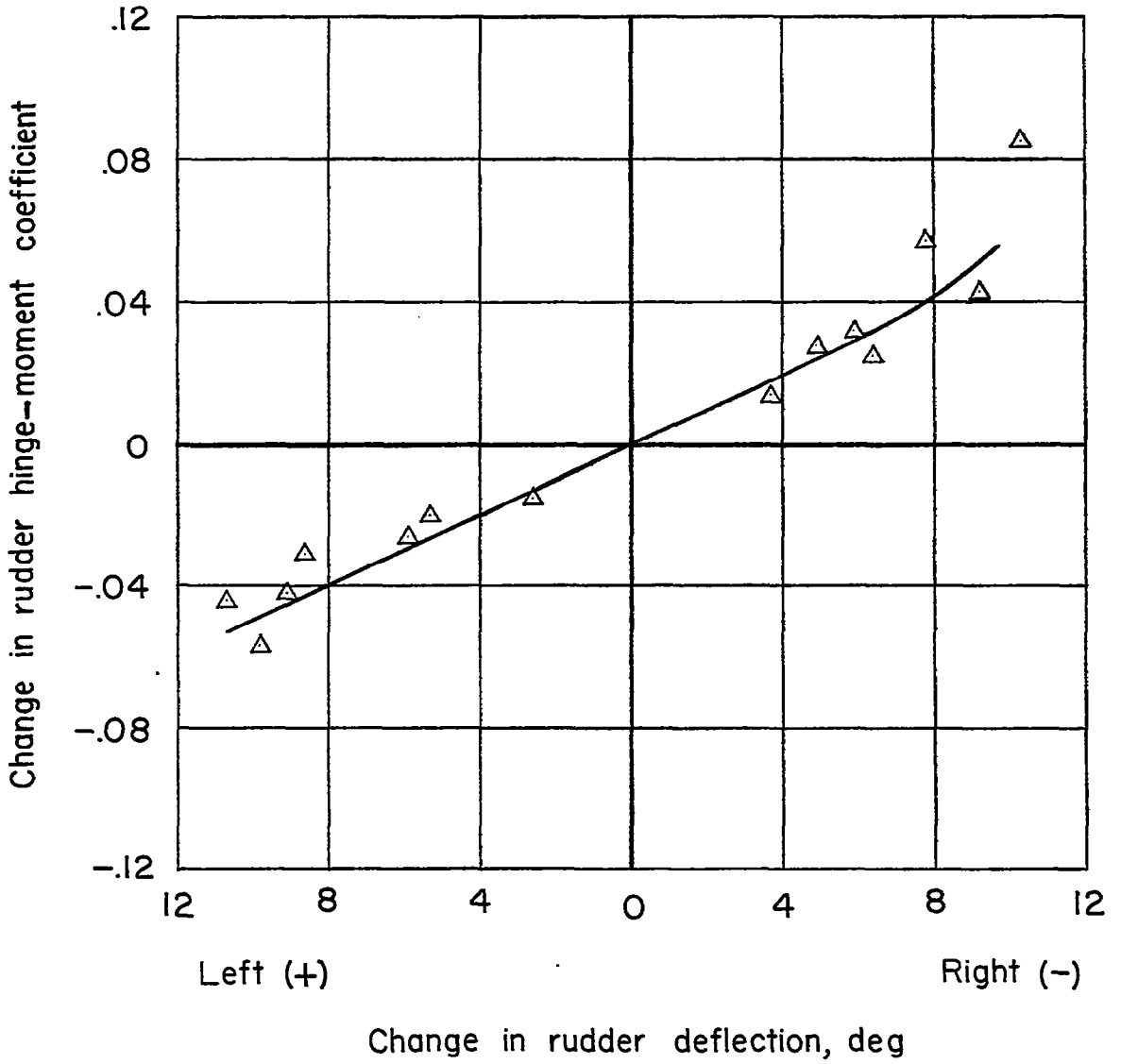

Figure 11.- Change in rudder hinge moment due to change in rudder deflection. First modification. Altitude, 10,000 and 30,000 feet; balancing tab ratio, 2:1; undamped, 1/8-inch-square rudder trailing-edge strips.

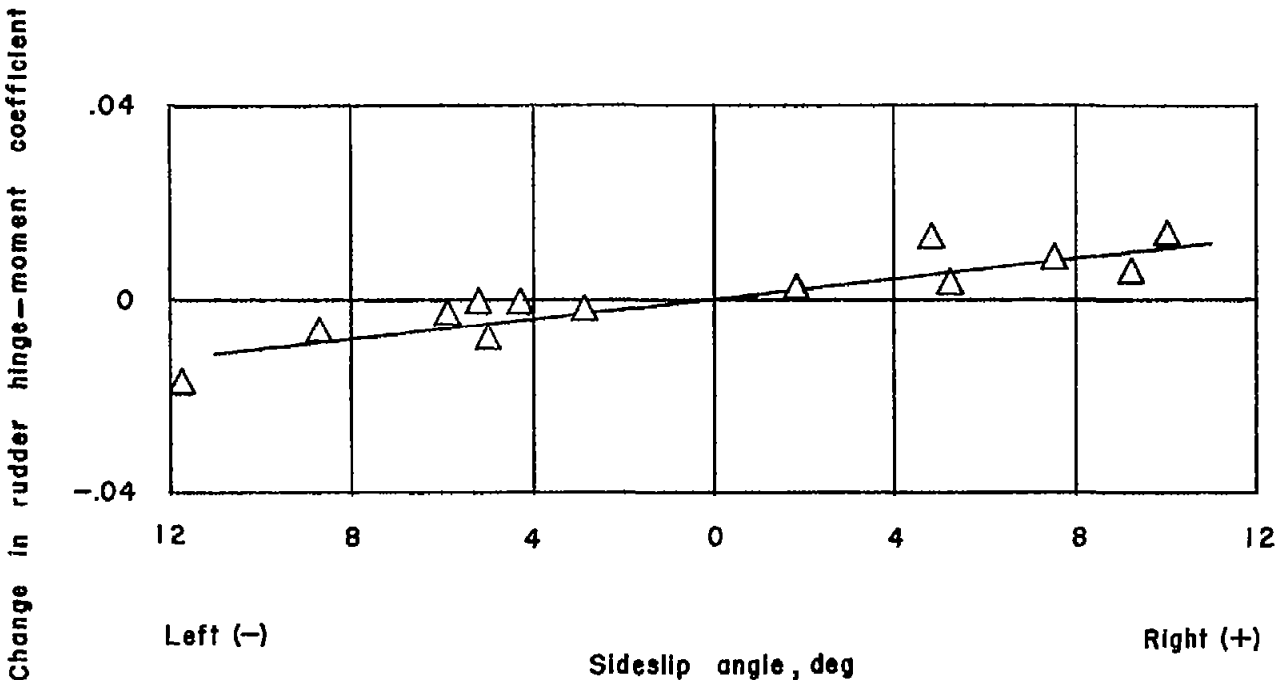

Figure 12.- Change in rudder hinge moment due to sideslip angle. First modification. Altitude, 10,000 and 30,000 feet; balancing tab ratio, 2:1; undamped 1/8-inch-square rudder trailing-edge strips.

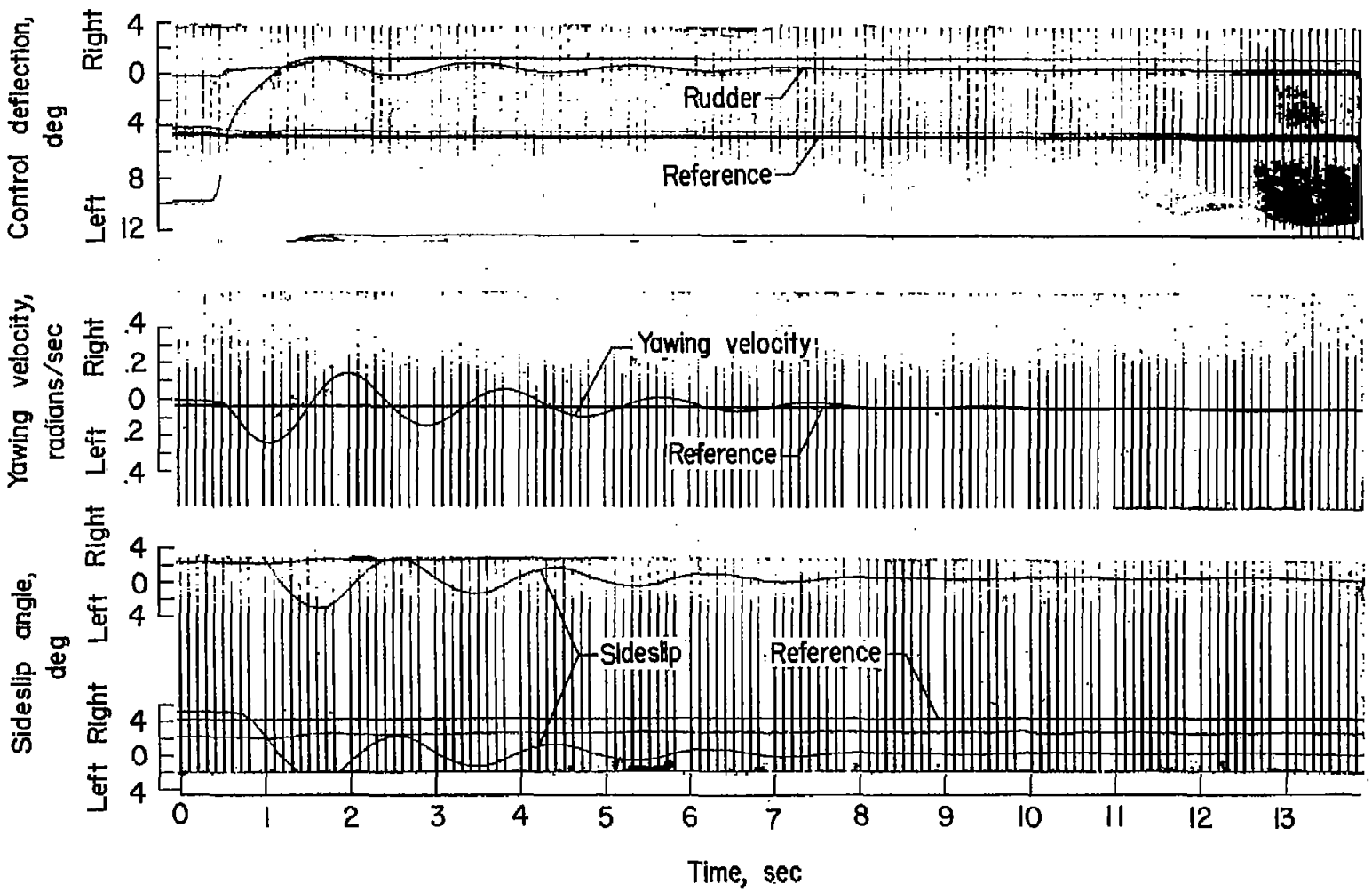

Figure 13.- Time history of lateral oscillation. First modification. M = 0.543; h_p = 10,000 feet; balancing tab ratio, 2:1; 1/8-inch-square rudder trailing-edge strips; viscous damper, 167 ft-lb/radian at 70° F.

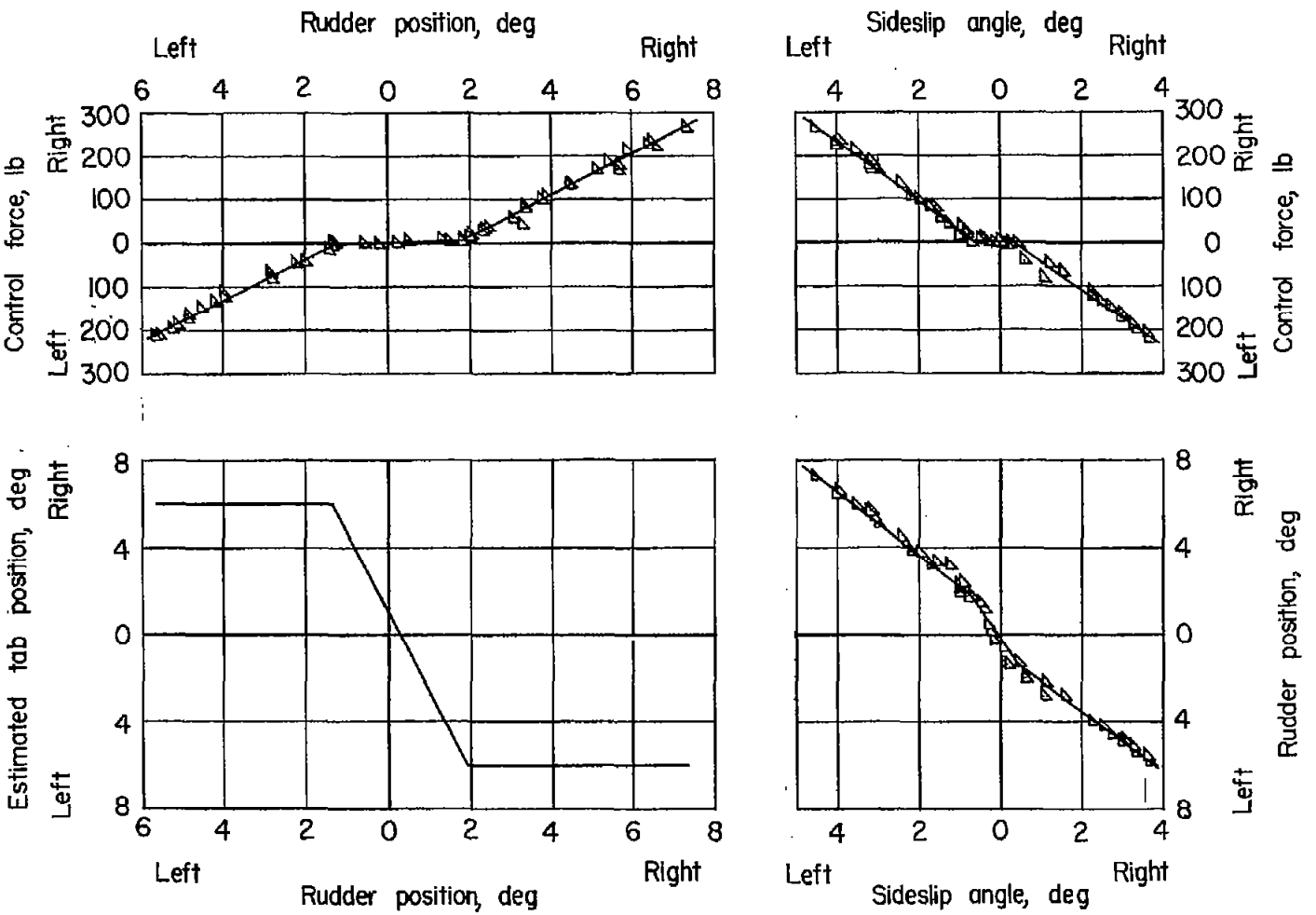

Figure 14.- Sideslip characteristics in clean condition from records of steady sideslips. Second modification. V_i = 275 knots; h_p = 10,000 feet; balancing tab ratio, 4:1; 5/16- by 1/4-inch rudder trailing-edge strips; viscous damper, 167 ft-lb/radian at 70° F.

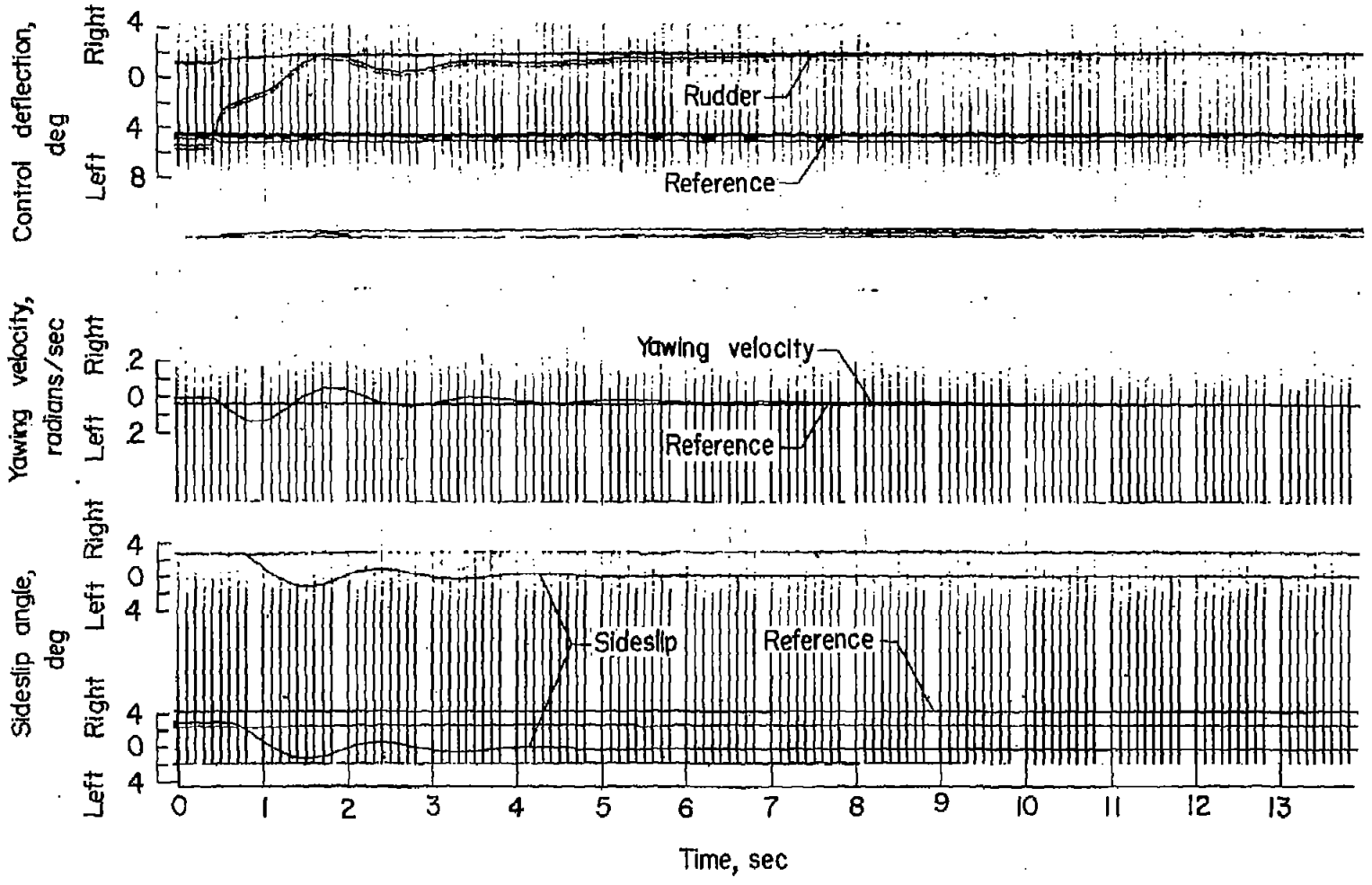

(a) $M = 0.537$; $h_p = 10{,}000$ feet.

Figure 15.- Time history of lateral oscillation. Second modification. Balancing tab ratio, 4:1; 5/16- by 1/4-inch rudder trailing-edge strips; viscous damper, 167 ft-lb/radian at 70° F.

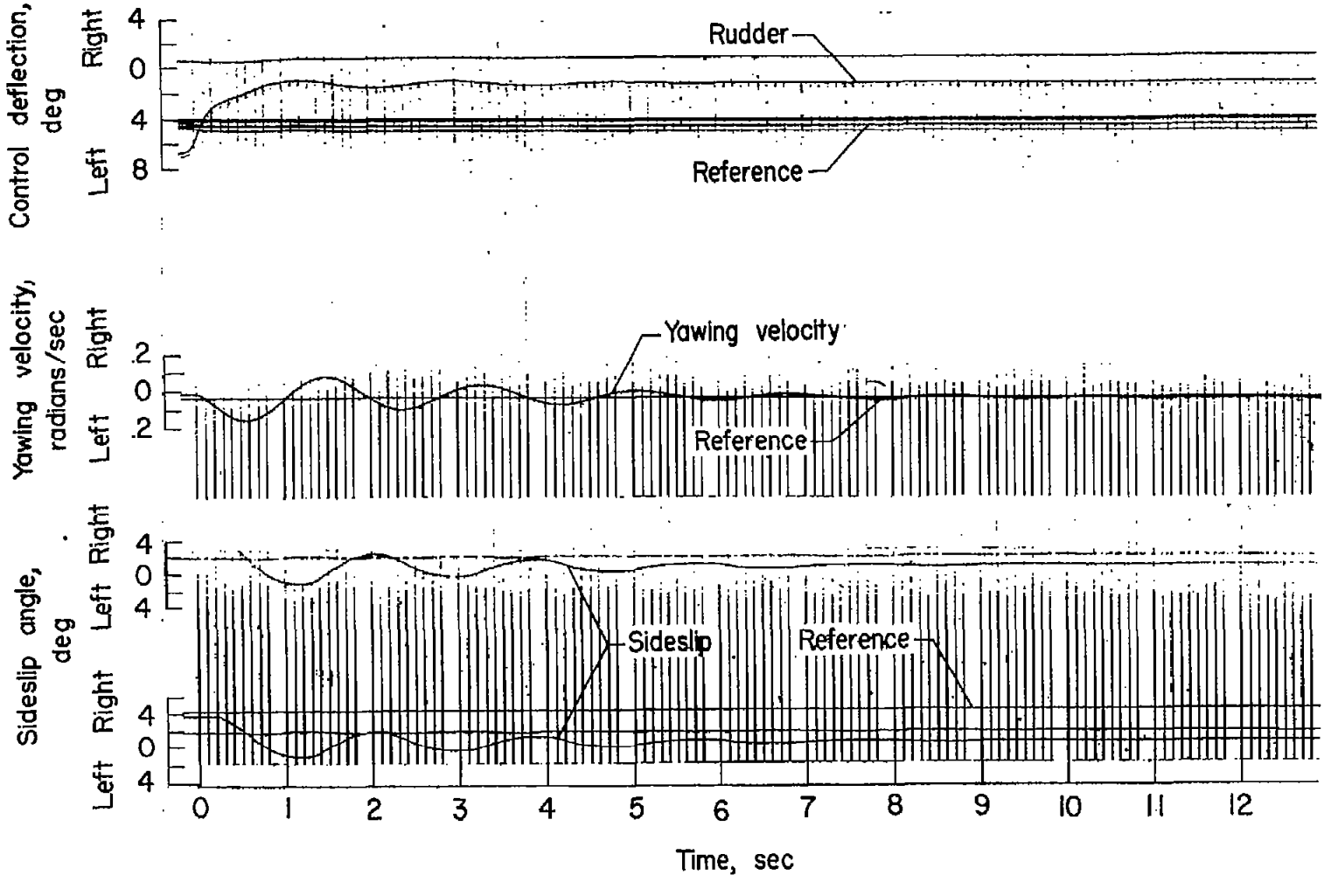

(b) $M = 0.76$; $h_p = 30{,}000$ feet.

Figure 15.- Concluded.

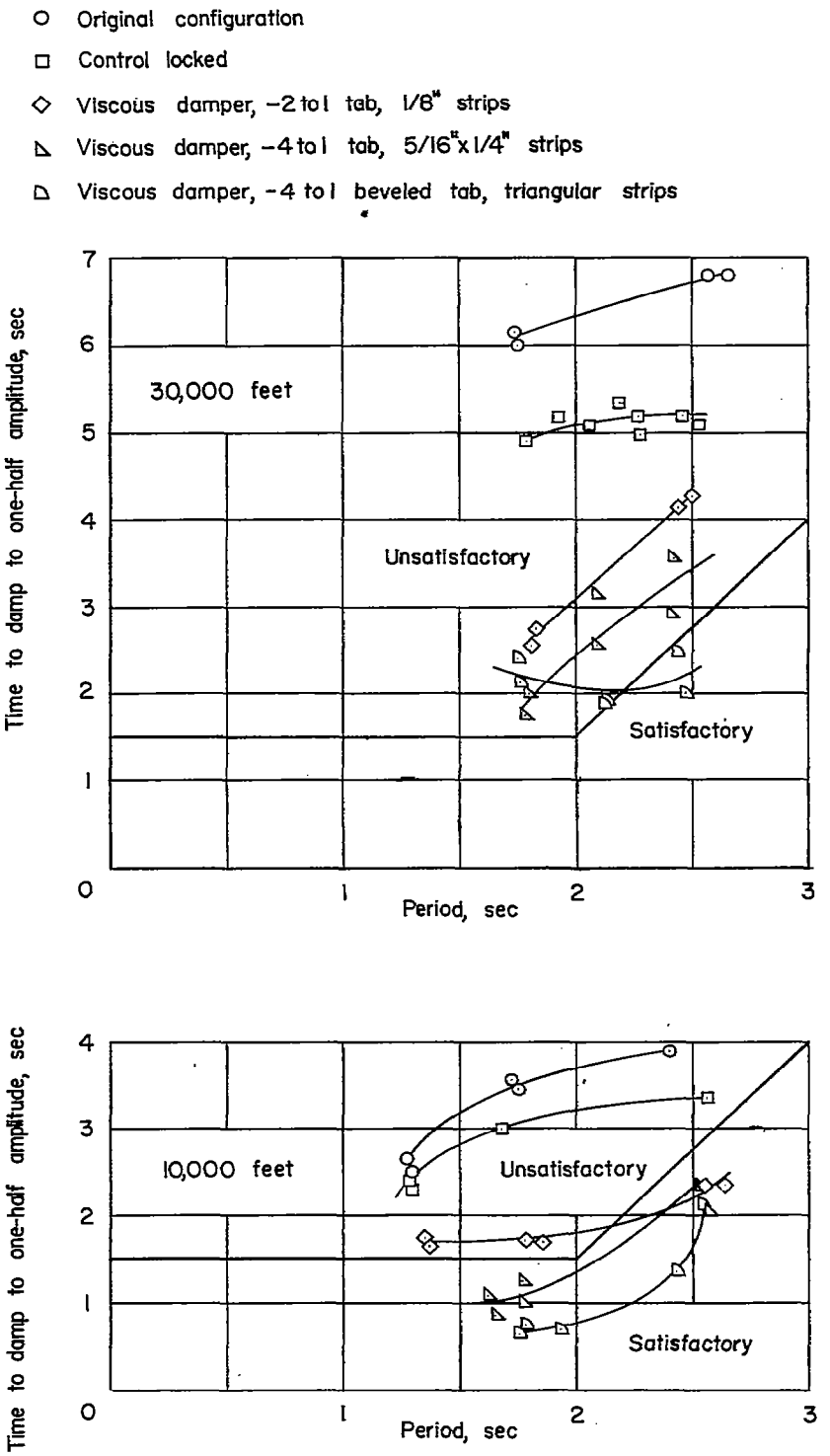

Figure 16.- Summary of measured damping of lateral oscillation. The boundary between satisfactory and unsatisfactory regions is that specified by the requirements of reference 4.

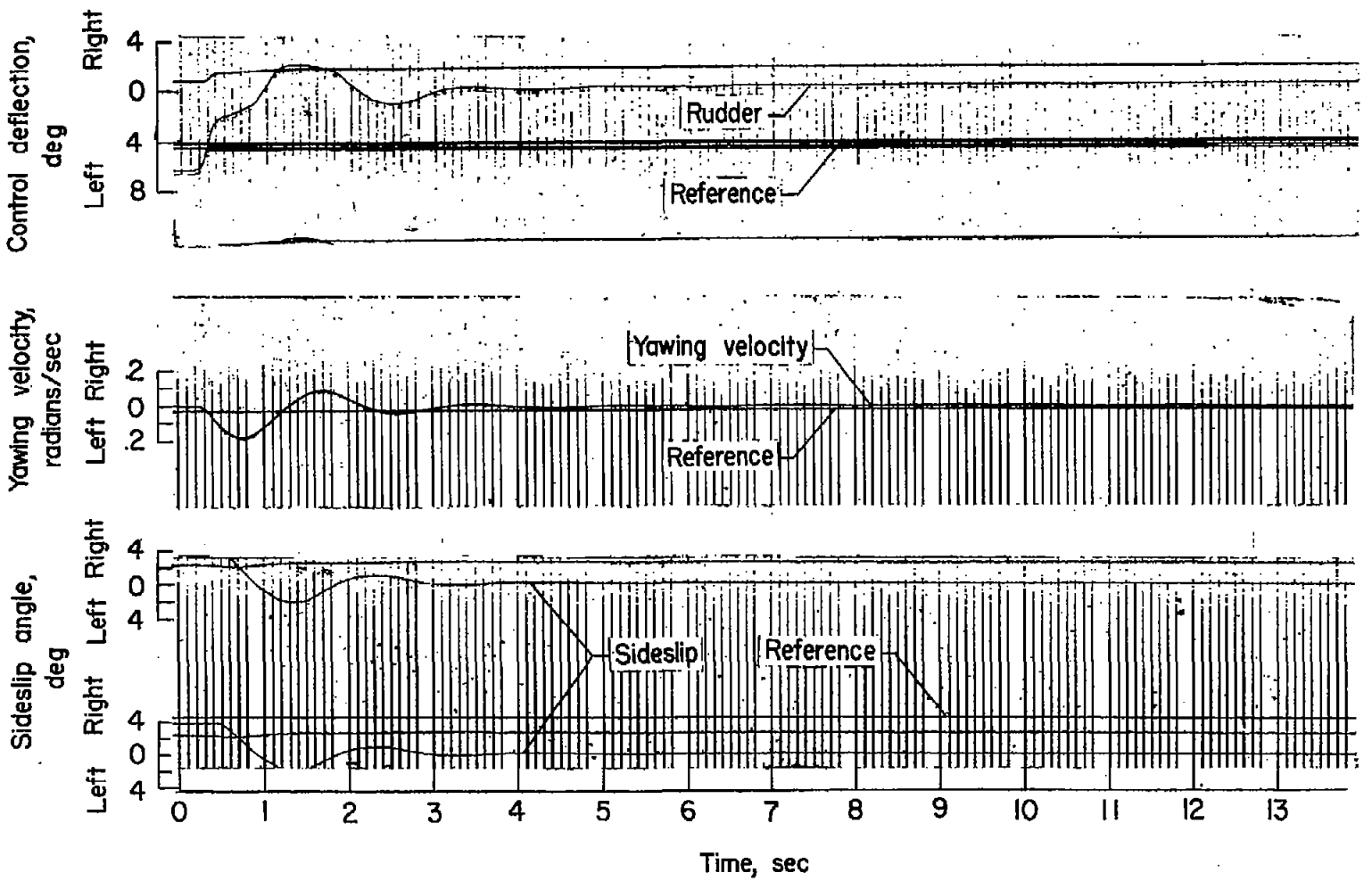

Figure 17.- Time history of lateral oscillation. Third modification. $M = 0.545$; $h_p = 10{,}000$ feet; balancing tab ratio, 4:1; triangular rudder trailing-edge strips; beveled rudder trim tab; viscous damper, 167 ft-lb/radian at 70° F.

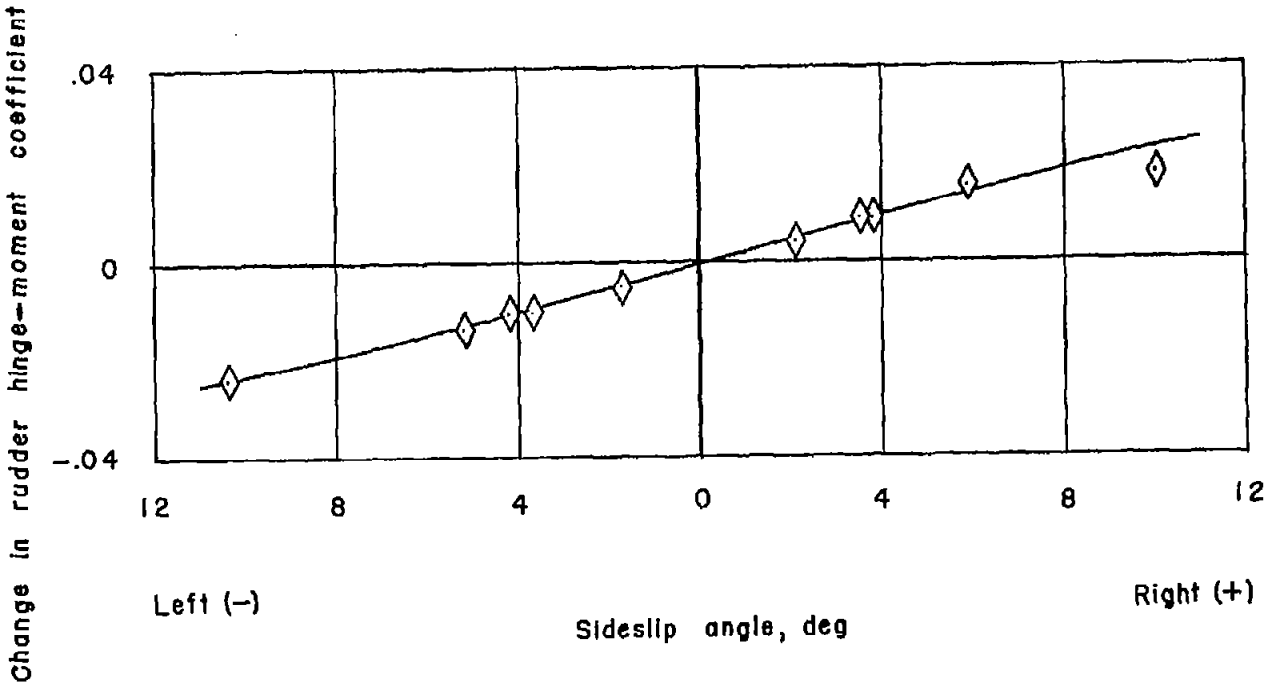

Figure 18.- Change in rudder hinge moment due to sideslip angle. Third modification. Altitude, 10,000 and 30,000 feet; balancing tab ratio, 4:1; triangular rudder trailing-edge strips; beveled rudder trim tab; viscous damper, 167 ft-lb/radian at 70° F.

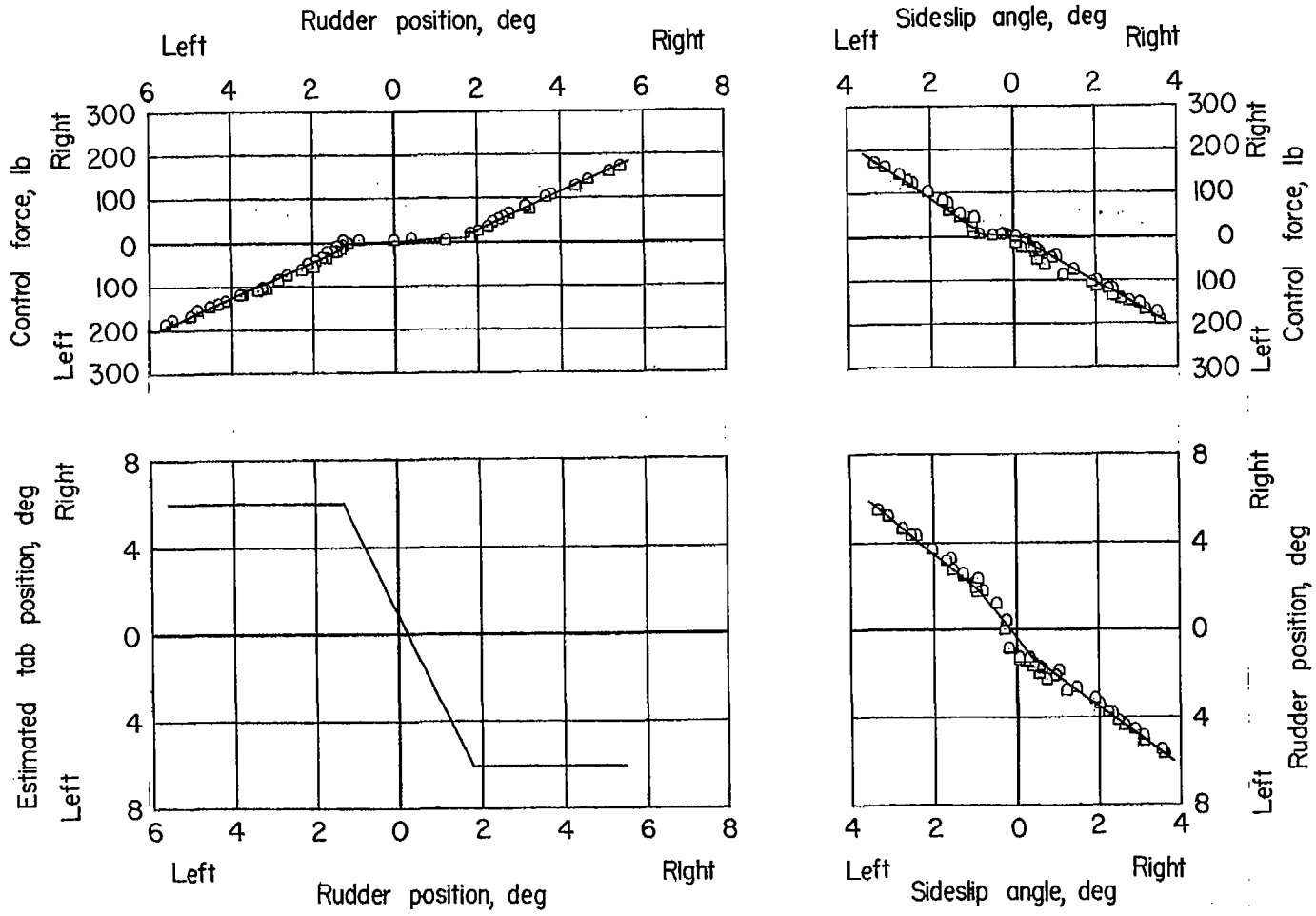

Figure 19.- Sideslip characteristics in clean condition from records of steady sideslips. Third modification. V_i = 275 knots; h_p = 10,000 feet; balancing tab ratio, 4:1; triangular rudder trailing-edge strips; beveled rudder trim tab; viscous damper, 167 ft-lb/radian at 70° F.

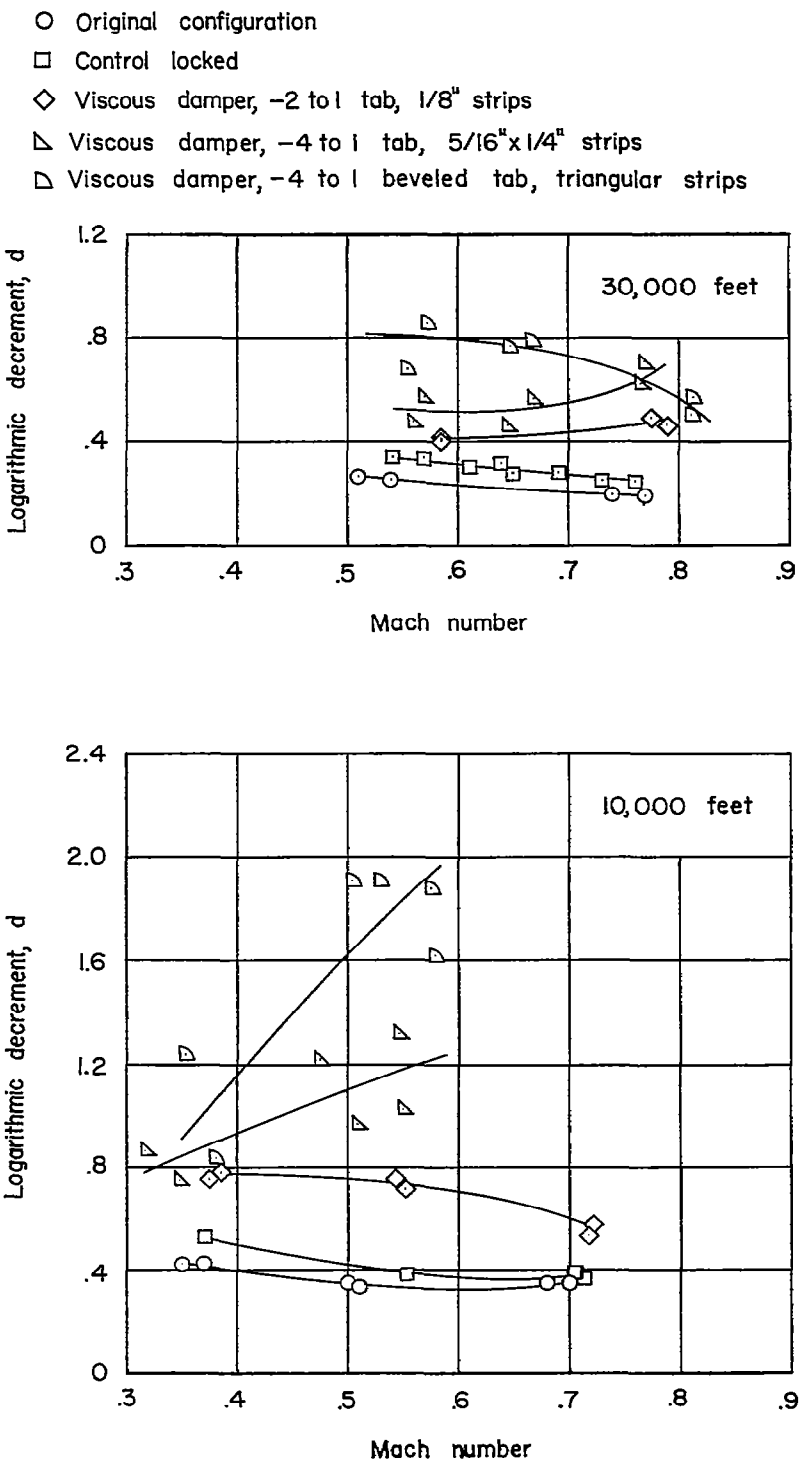

Figure 20.- Comparison of measured damping of lateral oscillation for various test configurations in terms of logarithmic decrement d.